Supplementary Information (SI) for Catalysis Science & Technology.
This journal is © The Royal Society of Chemistry 2026

Mild and efficient coupling reactions enabled by in situ electrolytically generated Cu(I) cation catalyst in nanoelectrospray

Annesha Sengupta[a], Gopal Reddy Ramidi[a], Disni Gunasekera[a], Mia Beaudoin[a], Shiqing Xu[a,b], and Xin Yan[a*]

[a] Department of Chemistry, Texas A&M University, College Station, Texas 77843, USA

[b] Department of Pharmaceutical Sciences, Texas A&M University, College Station, TX, USA

*Corresponding author: xyan@tamu.edu

Table of contents:

S1. NanoESI emitter fabrication and MS parameters:

NanoESI emitters were made from borosilicate glass capillary (1.5mm OD) from WPI Inc. (Sarasota, FL) with a P-1000 micropipette puller from Sutter Instrument Company (Novato, CA). The following parameters were used to obtain an orifice size of ~ 40 µm: Ramp: 646, Heat 640, Pull 0, Velocity 30, Time 250, and Pressure 500.

MS data were acquired on an Orbitrap Velos mass spectrometer (Thermo Fisher Scientific, San Jose, CA, USA) for both the low-resolution Ion Trap mode (IT-MS) and for the high-resolution Fourier Transform mode (FT-MS) with a resolution of 60,000.

A potential within the range of 2- 3.2 kV was applied to the Cu or Pt electrode depending on the experiment. The ion transfer capillary was held at 275°C for all analyses with S-lens RF level set to 67.9%. The distance between the nanoESI emitter tip and the mass spectrometer inlet was fixed at 0.7 mm to avoid microdroplet reaction and ensure accurate tracking of the reaction within the nanoelectrospray emitter while avoiding space charging effects. Full MS scans were acquired at various *m/z* ranges between *m/z* 50-500 in positive ion mode, 2 microscans, and a maximum injection time of 200 ms. The *m/z* ranges were optimized based on different reactions to enable accurate tracking of intermediates, products, and overall reactions over time. Tandem mass spectra (MS/MS) were obtained via collision-induced dissociation (CID), with normalized collision energy (NCE) ranging from 15-35 arbitrary units (arb), and an isolation window of 1.

MS data analysis was done using the Xcalibur Qual Browser program (Waltham, MA).

The continuous reaction progression of C–H amination of N-phenylpicolinamide with morpholine in the electrochemical Cu catalytic microreactor (in Fig. 3) was monitored using ion trap-MS. Each individual peak was confirmed in Full MS and tandem MS using high-resolution Fourier Transform mode (FT-MS) with a resolution of 60,000. The *m/z* reported precision in Figure 3 is as per the high-resolution confirmation to avoid any confusion.

The reaction time was controlled by the voltage application process. The voltage application drove two phenomena: a) Cu-mediated catalysis, and b) nanoelectrospray for online reaction monitoring. Stopping the voltage application stopped both our reaction and nanoelectrospray (hence stopping the online reaction and the monitoring simultaneously). The reaction times mentioned in this work refer to the duration of voltage application to the nanoESI microreactor.

All product assignments were made using a combination of high-resolution mass spectrometry (HRMS) and tandem mass spectrometry (MS/MS). Further, these were confirmed with standard products. The exact mass and fragmentation patterns of the detected species were matched against independently synthesized reference compounds, providing high-confidence structural validation. We have added the following information in specified Supplementary sections.

C-H Amination Reaction: Product of CH Amination reaction, **3**, *N*-[2-(4-Morpholinyl)phenyl]benzamide was confirmed by HRMS, Tandem MS, ^{1}H NMR and ^{13}C NMR (Fig. S13, Fig. S16-S17, Fig. S32-34).

N–N homocoupling of *o*-phenylenediamine: The product was characterized in situ in nanoESI-MS by exact mass match with HRMS (with Δ ppm reported for theoretical versus observed exact mass), and structural confirmation via tandem MS in HRMS (Fig. S21, Fig. S23, Table S3).

Dehydrogenative intramolecular N–N coupling of anthranilamide: The product was characterized in situ in nanoESI-MS by exact mass match with HRMS (with Δ ppm reported for theoretical versus observed exact mass), and structural confirmation via tandem MS in HRMS (Fig. S27-28, Table S6). Further, purchased reference compound 3-Indazolinone was used as a standard for product identification **7** using HR-MS and tandem MS (Fig. S26 d)

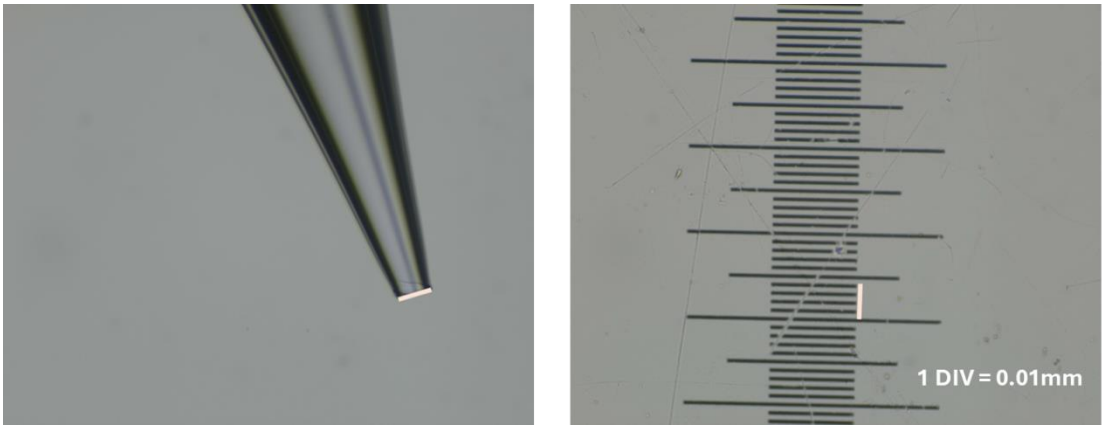

Fig. S1 Microscopic image of nanoESI emitter made from borosilicate glass capillary (1.5mm OD) pulled with a P- 1000 micropipette puller from Sutter Instrument Company to obtain an orifice size of ~ 40 µm.

S2. Optimal voltage for anodic corrosion and electro dissolution of Cu cations in nanoESI

Cu(I)-cation generation: The purpose of the 0.02 kV experiment was to detect the minimum threshold for catalytic Cu(I) generation within the nanoelectrospray emitter. By applying this low voltage without generating an electrospray, we confirmed that Cu(I) cations are produced via anodic corrosion and electrodissolution governed by standard electrochemical (SHE) parameters. This proves that the catalyst is generated through predictable electrochemical pathways and is not an artifact of the high-voltage electrospray conditions or gas-phase ion chemistry.

Nanoelectrospray Microreactor Conditions: While 0.02 kV is sufficient for the chemical dissolution of the Cu electrode, a higher voltage (2–3 kV) is required in the actual nanoESI microreactor setup to overcome surface tension and generate the electrospray plume. This higher operational voltage ensures a continuous flow of reactants to the mass spectrometer for online monitoring and real-time kinetic capture.

This low-voltage study is a foundational control experiment intended to validate the electrochemical nature of the catalyst source prior to its integration into the high-voltage microreactor environment.

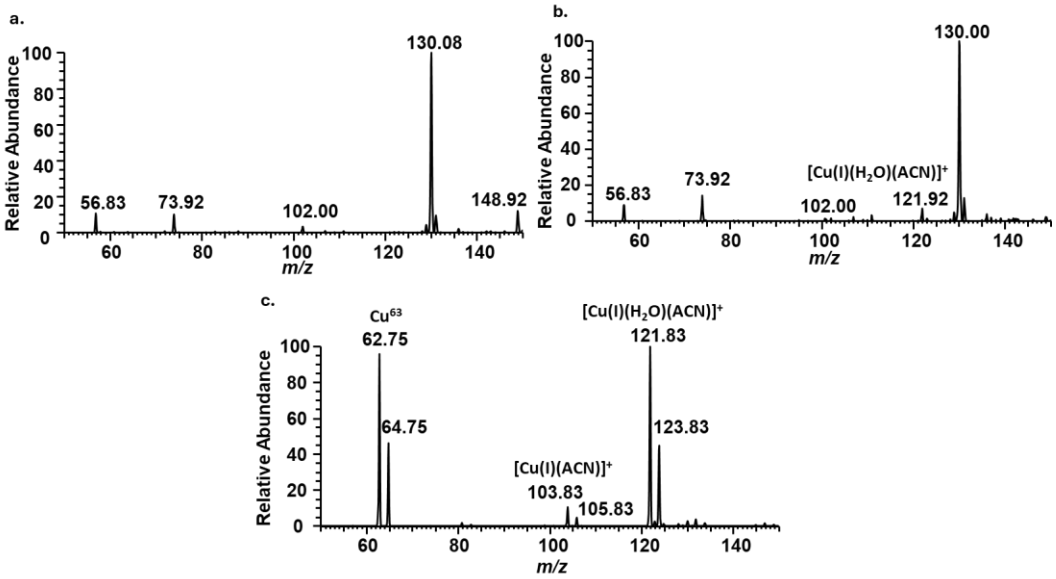

Fig S2. For determination of optimal voltage in nanoESI for Cu anodic corrosion and electrodissolution, a Cu electrode was inserted in a nanoESI emitter containing ACN solution and different voltage was applied for different length of time. The Cu electrode was then replaced by Pt electrode in the emitter and 1.5kV was applied to transfer the emitter solution to the mass spectrometer for detecting Cu-ligand complexes. Full MS showing detection of emitter solution, a. 0.01kV applied to Cu electrode for 30 seconds showing only background peaks, b. 0.01kV applied to Cu electrode for 1 min showing detection of a small peak of $Cu(I)(H_2O)(ACN)]^+$ at m/z 122.0, c. 0.02kV applied to Cu for 1 min showing dominating Cu(I)-cation peak at *m/z* 63.0, of Cu-adducted ligand peaks of $[Cu(I)(ACN)]^+$ at m/z 104.0, and $Cu(I)(H_2O)(ACN)]^+$ at m/z 122.0 indicating the optimal voltage for Cu anodic corrosion, electrodissolution, and detection of Cu-ligand complexes in nanoESI.

S3. Electrolytic in situ generation of Cu cations in nanoESI

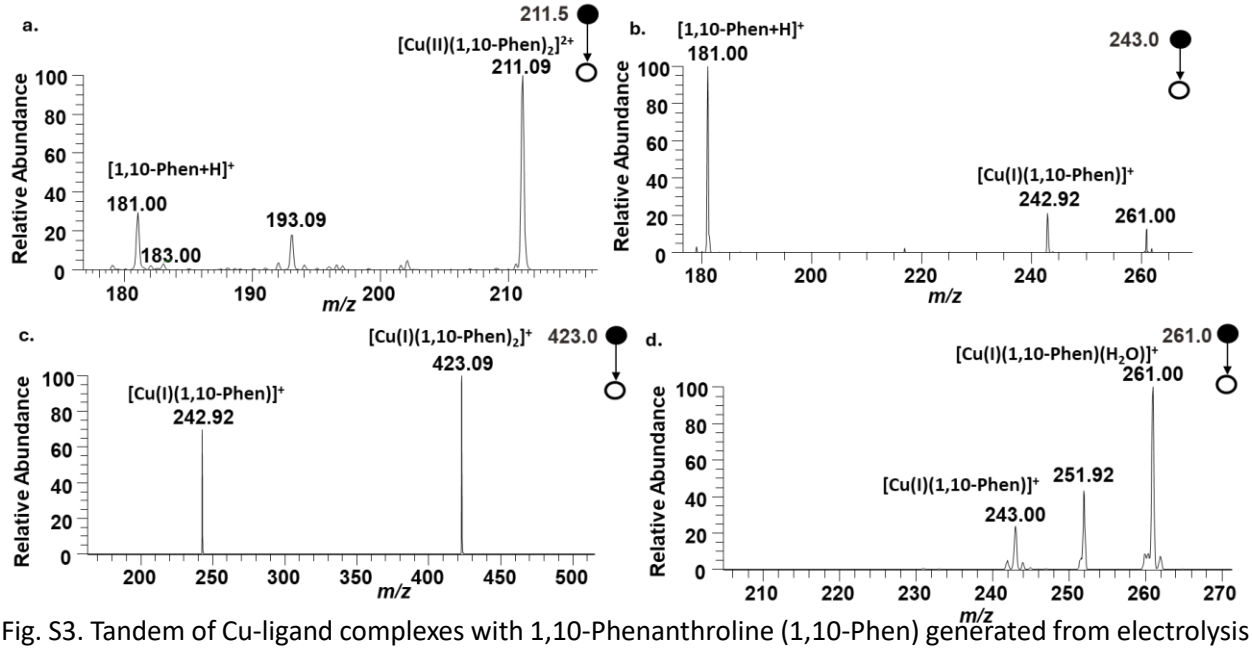

Fig. S3. Tandem of Cu-ligand complexes with 1,10-Phenanthroline (1,10-Phen) generated from electrolysis of Cu electrode in nanoESI a. $[Cu(II)(1,10\text{-}Phen)_2]^{2+}$ at m/z 211.5, b. $[Cu(I)(1,10\text{-}Phen)]^+$ at m/z 243.0, c. $[Cu(I)(1,10\text{-}Phen)_2]^+$ at m/z 423.0. d. $[Cu(I)(1,10\text{-}Phen)(H_2O)]^+$ at *m/z* 261.0

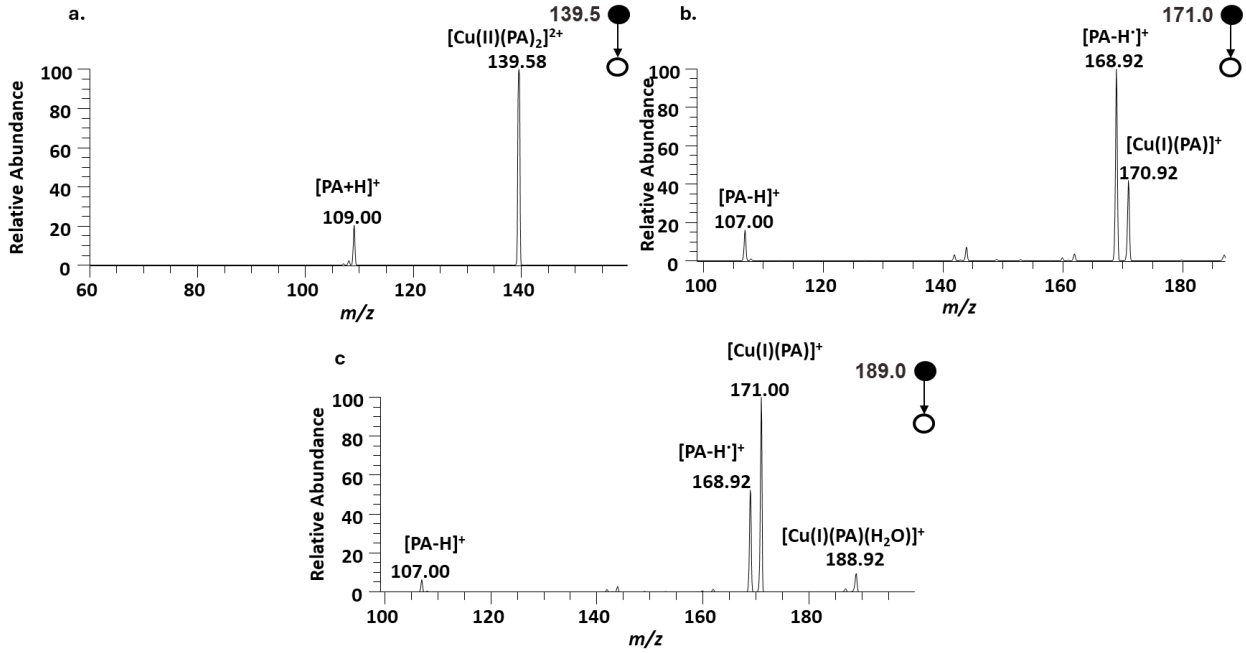

Fig. S4. Tandem of Cu-ligand complexes with In 2-Picolylamine (PA) from electrolysis of Cu electrode in nanoESI. a. $[Cu(II)(PA)_2]^{2+}$ at *m/z* 139.5, b. $[Cu(I)(PA)]^+$ at *m/z* 171.0, and c. $[Cu(I)(PA)(H_2O)]^+$ at *m/z* 189.0

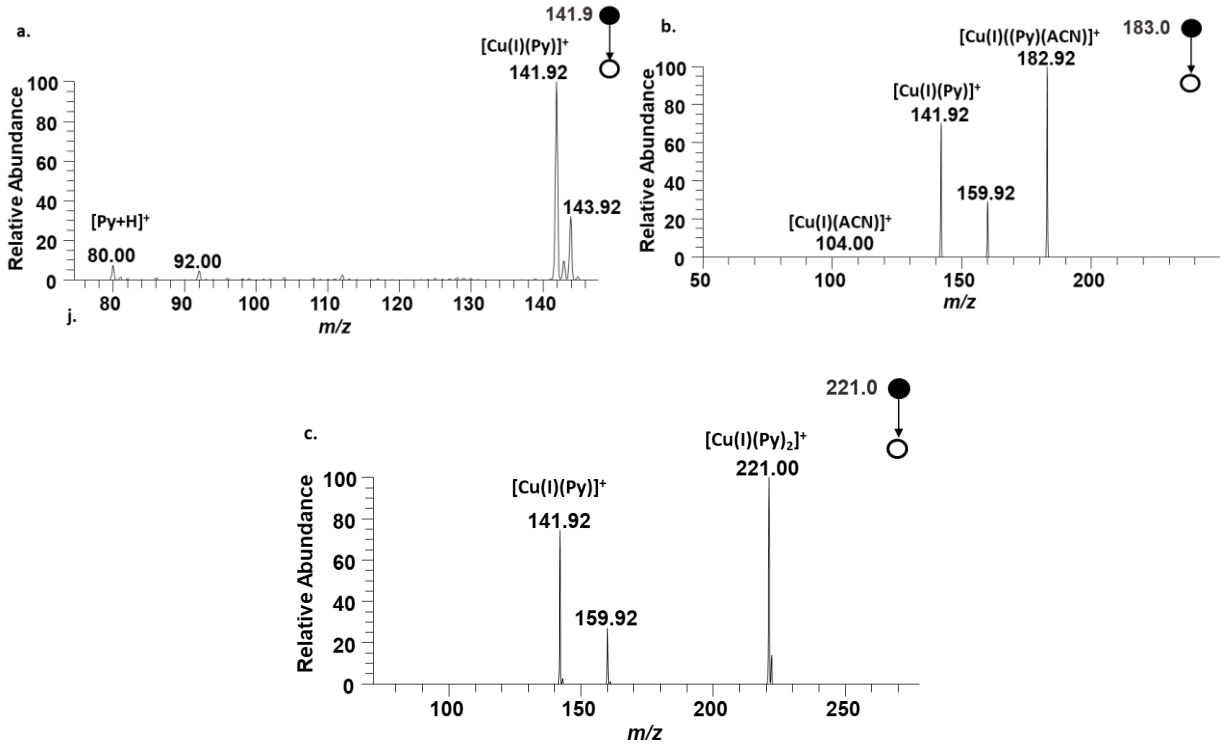

Fig. S5. Tandem of Cu-ligand complexes with Pyridine (Py) in acetonitrile (ACN) generated from electrolysis of Cu electrode in nanoESI a. $[Cu(I)(Py)]^+$ at m/z 141.9, b. $[Cu(I)(Py)(ACN)]^+$ at m/z 183.0, and c. $[Cu(I)(Py)_2]^+$ at m/z 221.0

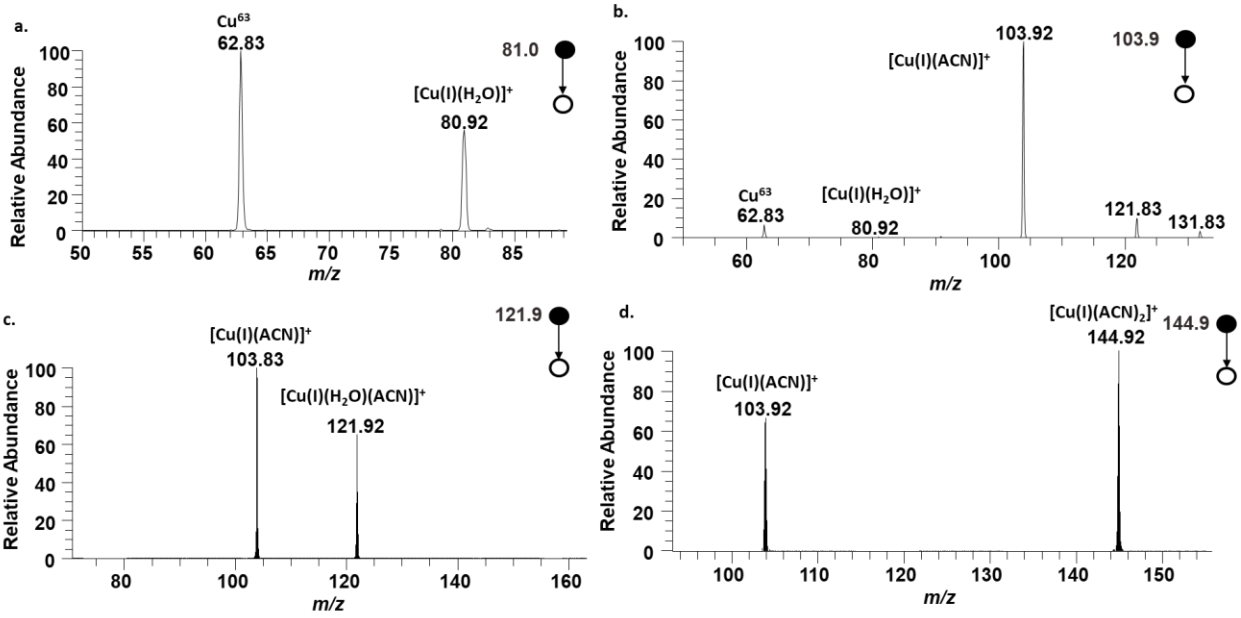

Fig. S6. Tandem of Cu-ligand complexes with acetonitrile (ACN) generated from electrolysis of Cu electrode in nanoESI a. $[Cu(I)(H_2O)]^+$ at m/z 81.0, b. $[Cu(I)(ACN)]^+$ at m/z 104.0, c. $[Cu(I)(H_2O)(ACN)]^+$ at m/z 122.0, and d. $[Cu(I)(ACN)_2]^+$ at m/z 144.9

We also compared the spectra obtained from electrospraying a Cu(II)Cl_2 solution (50 µM in ACN) using a platinum electrode with those that produced from Cu electrode corrosion in ACN (Fig. 2e). The resulting mass spectrum was identical to each other, indicating that Cu(II) ions are reduced to Cu(I) during the ESI process. Isotopic distribution patterns and tandem MS analyses (Fig. S3–S6) confirmed the identities and oxidation states of these Cu complexes. This gas-phase reduction likely arises from charge transfer and ligand desolvation events occurring within the spray plume.[44,48] This observation aligns with previously established literature that the high-energy desolvation and entropic changes during electrospray frequently compromise the stability of kinetically labile Cu(II) coordination complexes, favoring their reduction to Cu(I).[59] This observation suggests the high preference of the nanoelectrospray environment for catalytically active Cu(I) species. This also serves as a diagnostic baseline for our mechanistic study where we observe the sequential appearance of high-valent Cu(II) and Cu(III) species in reaction kinetic profiles which are inherently more stable even under high-energy gas phase desolvation events of nanoelectrospray, suggesting the observation of covalently bonded organometallic intermediate species formed during the catalytic cycle and not merely gas phase mass spectrometric adducts or labile coordination complexes.

This work emphasizes on Cu(I) as a major Cu-cationic species and primary catalytic contributor of all reactions. This is because, as observed in this study and reported in previous studies of anodic corrosion of Cu in nanoelectrospray settings, the presence and dominance of Cu(I) cations is a result of comproportionation reaction. Cu(0) to Cu(II) oxidation via electrolysis follows a Mattson and Bockris mechanism, where Cu(I) detachment process from metal is considered faster, whereas the second oxidation step is slower involving the oxidation of a hydrated species. Thus, Cu(I) ions electrogenerated in these conditions can react directly with ligands.[60]

S4. Concentration of in situ electrolytically generated Cu cations in nanoESI

Due to the continuous flow of solution in the nanoelectrospray microreactor, the system exhibits heterogeneous Cu concentrations caused by the ongoing electrolytic generation of Cu species at the electrode and their subsequent consumption as they are sprayed into the mass spectrometer for kinetic capture. Because the copper is being continuously removed from the system, reporting a traditional batch-wise catalytic turnover is not feasible. Instead, we report an estimated instantaneous concentration of the Cu(I)-cations present in the nanoelectrospray solution at the specific time of product formation (t).

We measured the concentrations of in situ electrolytically generated Cu(I) species by external calibration. The calibration curve was generated using 1, 2.5, 5, 10, 20, 50, and 100µM Cu(I)Cl salt in Acetonitrile solvent (where ACN functioned both as solvent). Total ion intensities of Cu(I) species of Cu+ at *m/z* 63, and Cu-ACN adducts $[Cu(I)(H_2O)]^+$ (*m/z* 81.08), $[Cu(I)(ACN)]^+$ (*m/z* 104.08), $[Cu(I)(H_2O)(ACN)]^+$ (*m/z* 122.00), and $[Cu(I)(ACN)_2]^+$ (*m/z* 144.92) (Fig. 2d) were normalized against the signal of intrinsic reaction matrix of [TEA]+ signal at *m/z* 130.08. Normalized ion intensities of the Cu(I)-species were plotted against Cu(I)Cl concentrations. The Cu(I)-ion concentration was calculated to be 2.44µM, 2.51µM, and 32.7µM at 1, 4 and 15 min of voltage application. This corresponds to 1.22 mol % of **6** for N-N intramolecular dehydrogenative coupling of anthranilamide (200µM, t= 1min), 5.02 mol% of **4** for N–N homocoupling of *o*-phenylenediamine (50µM, t= 4min), and 13.09 mol% of **1** for C-H Amination (250µM, t= 15 min).

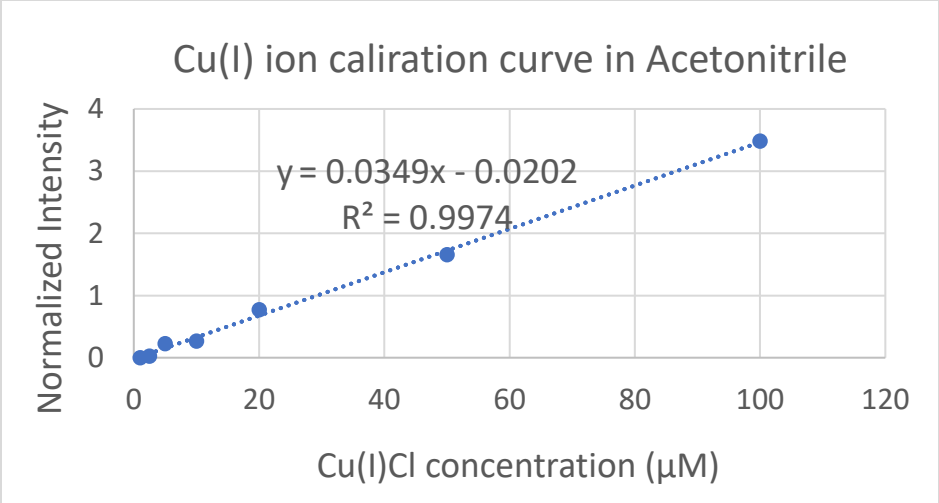

Fig. S7 Normalized MS intensities of Cu(I)ions versus the concentration of Cu(I)Cl salt in Acetonitrile

S5. Mild and efficient Cu-catalyzed online electrochemical C-H amination

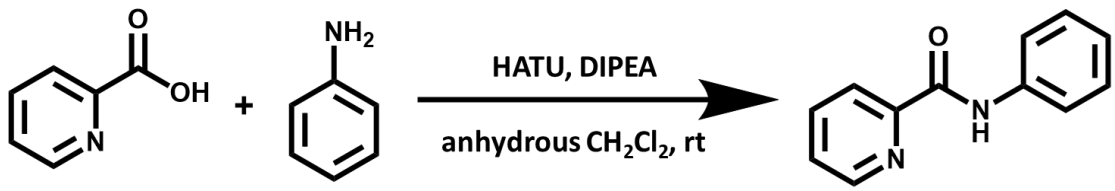

Fig. S8. A mixture of aniline (0.93g, 10mmol, 1.0 eq.), picolinic acid (1.35g, 11mmol, 1.1 eq.) , HATU (4.18g, 11mmol, 1.1 eq.), DIPEA (5.20 mL, 30 mmol, 3.0 eq.), in anhydrous CH_2Cl_2 (20 mL), was stirred at room temperature overnight. Water was added and the mixture was extracted with CH_2Cl_2. The combined organic layers were washed with water and brine, and dried over anhydrous sodium sulfate, and concentrated in rotavapor. The resulting residue was purified by silica gel flash chromatography in 60% EtOAc /40% hexane to get the desired *N*-Phenylpicolinamide product.

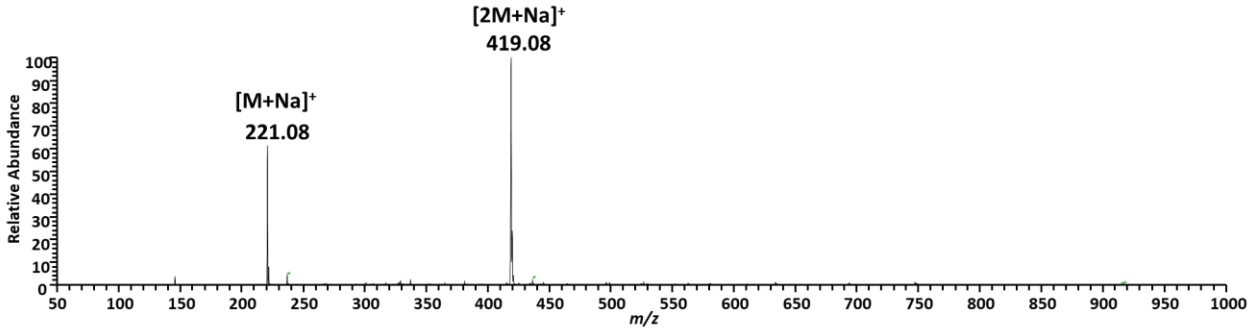

Fig. S9. MS of *N*-Phenylpicolinamide after purification by silica gel flash chromatography with peaks of detected $[M+Na]^+$ at *m/z* 221.08 and $[2M+Na]^+$ at *m/z* 419.08

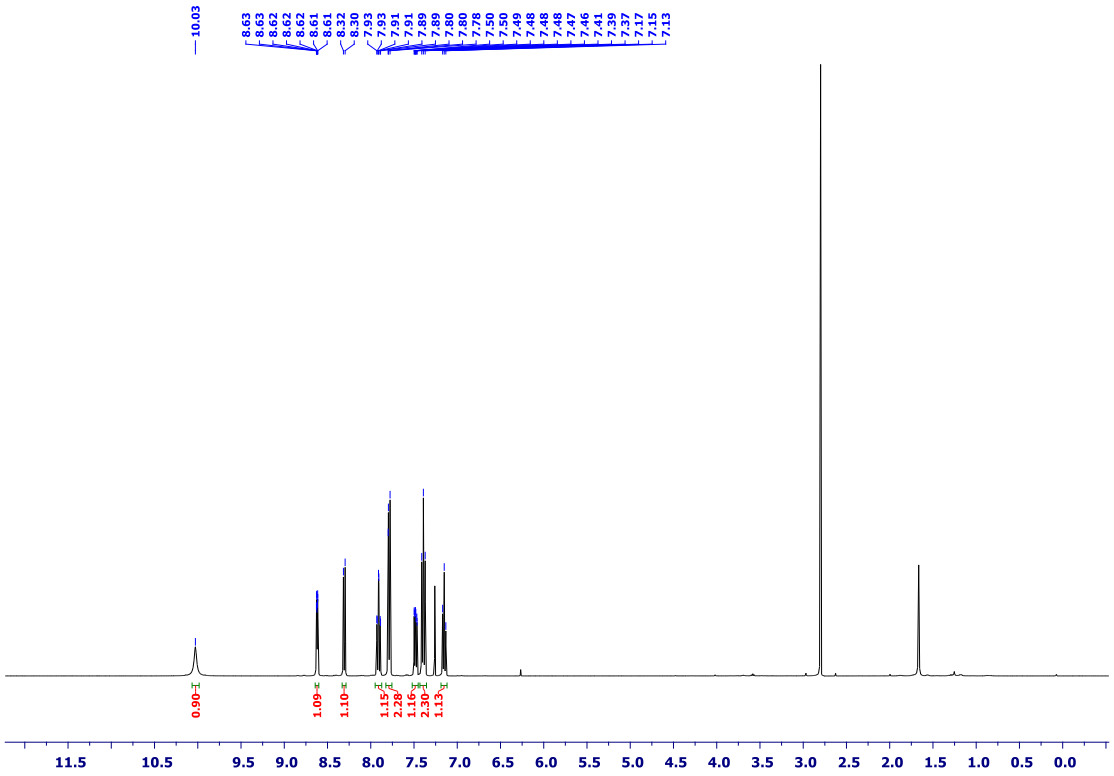

^{1}H NMR (400 MHz, $CDCl_3$) δ 10.03 (s, 1 H), 8.61-8.63 (m, 1 H), 8.30-8.32 (m, 1 H), 7.91 (td, *J*= 7.91 Hz,1 H), 7.78-7.80 (m, 2 H), 7.46-7.50 (m, 1 H), 7.31 (t, *J* = 7.4 Hz, 2 H), 7.15 (t, *J* = 7.16 Hz, 1 H) ppm

Fig. S10. NMR of *N*-Phenylpicolinamide after purification by silica gel flash chromatography

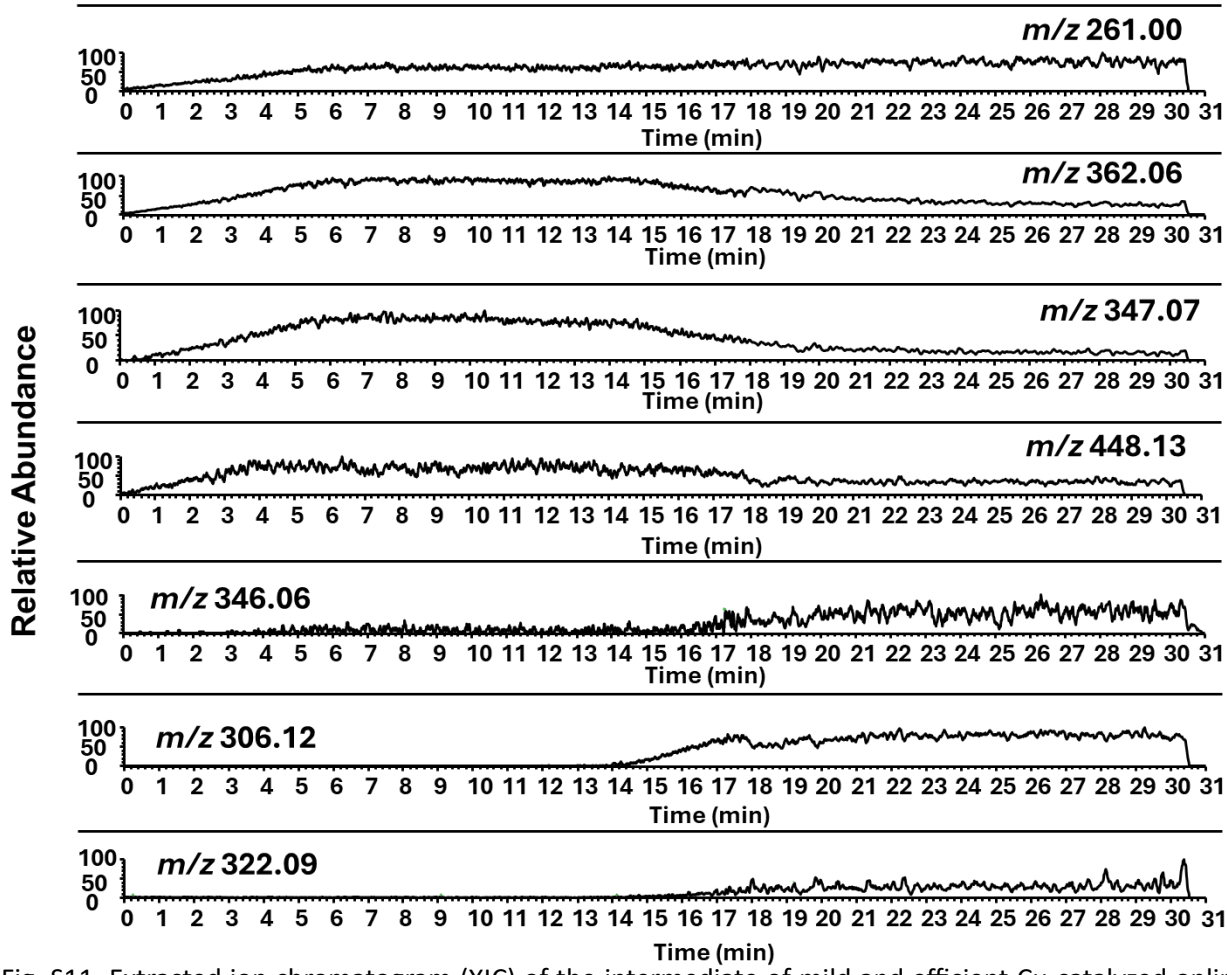

Fig. S11. Extracted ion chromatogram (XIC) of the intermediate of mild and efficient Cu-catalyzed online electrochemical C-H amination. The XIC of intermediates at *m/z* 261.01*, m/z* 362.06, *m/z* 347.07, *m/z* 448.13, shows increased stabilized intensity around 4 minutes; their concentration gradually decreases from 16 to 30 minutes when product peaks, bound to Cu(I) *m/z* 346.06, adducted to Na *m/z* 306.12, and K *m/z* 322.09 show increasing concentrations over time from 16 to 30 minutes.

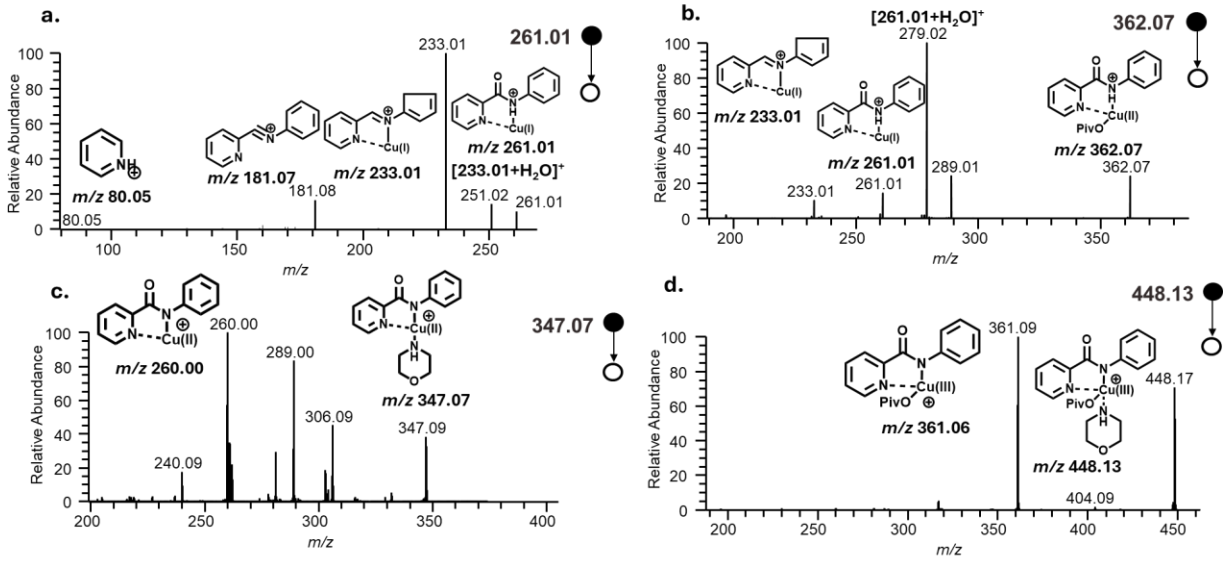

Fig. S12. Tandem of intermediates of mild and efficient Cu-catalyzed online electrochemical C-H amination of: a. Cu(I)-intermediate $\mathbf{I_1}$ (*m/z* 261.01), b. Cu(II)-intermediate $\mathbf{I_2}$ (*m/z* 362.07), c. Cu(II)-intermediate $\mathbf{I_3}$ (–OPiv) (*m/z* 347.07), d. Cu(III)-intermediate $\mathbf{I_4}$ (-Iodide) (*m/z* 448.13)

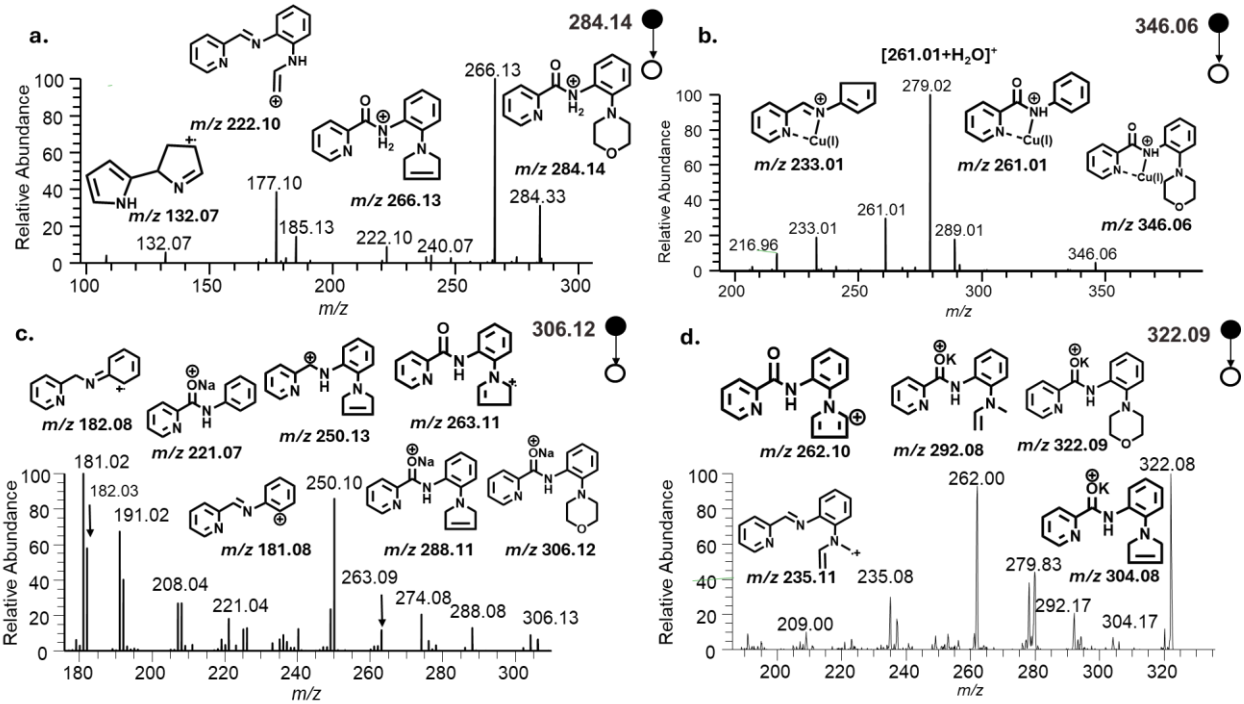

Fig. S13. Tandem of product and C-N coupled intermediate peaks from online synthesis of C-H amination of *N*-phenylpicolinamide with morpholine. a. FT-MS/MS of [**3**+H]$^+$ (*m/z* 284.14), b. FT-MS/MS of $\mathbf{I_6}$ [Cu(I)(3-H)+H]$^+$ (*m/z* 346.06), c. IT-MS/MS of [**3**+Na]$^+$ (*m/z* 306.12), d. IT-MS/MS of [**3**+K]$^+$ (*m/z* 322.09). Product fragmentations match with the tandem-MS of the bulk synthesis product peaks (at *m/z* 284.14, *m/z* 306.12, and *m/z* 322.09 that were confirmed with HRMS in full MS) (Fig. S15-S16)

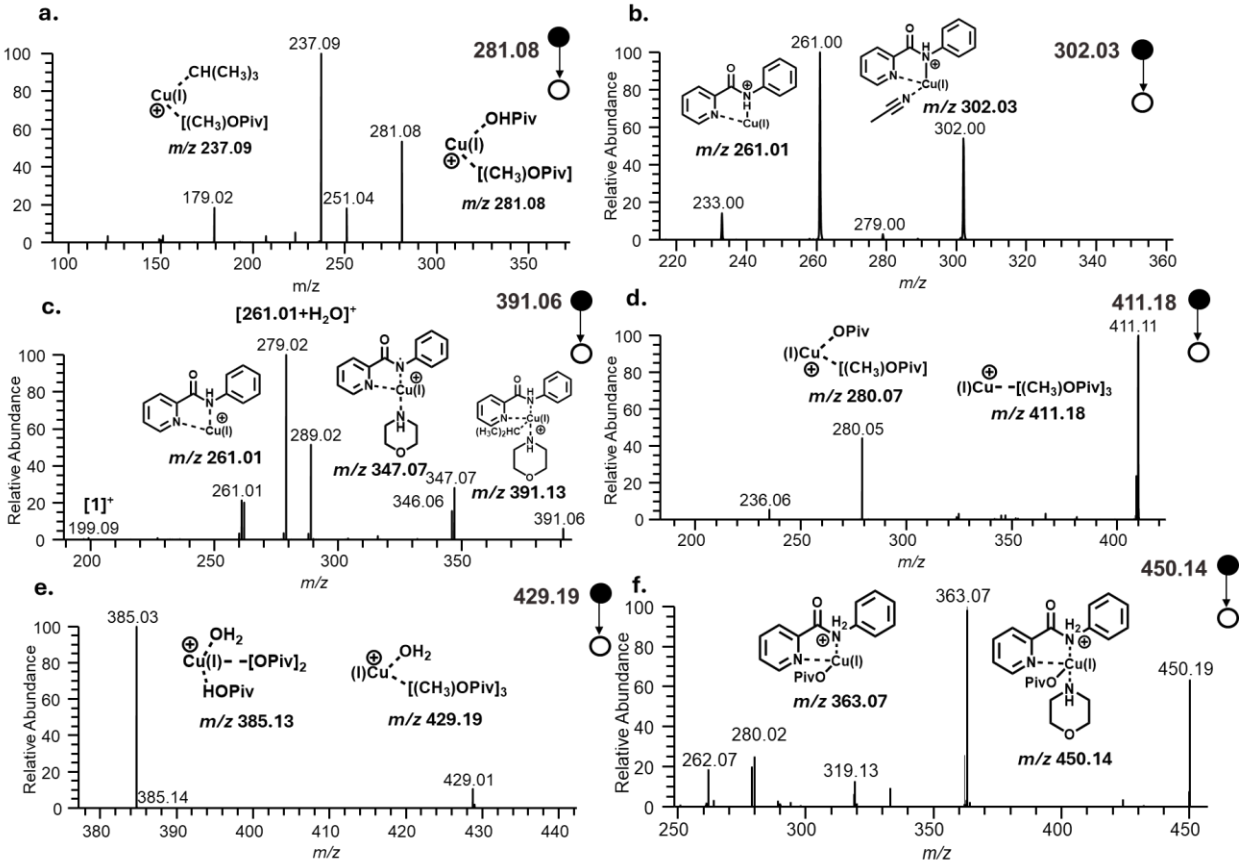

Fig. S14. Tandem of Cu(I)-adducts: a. $[Cu(I)(HOPiv)(CH_3OPiv)]^+$ (*m/z* 281.08) b. $[Cu(I)(1)(ACN)]^+$ (*m/z* 302.03), c. $[Cu(I)(1)(2)(CH(CH_3)_2]^+$ (*m/z* 391.06), d. $[Cu(I)(CH_3OPiv)_3]^+$ (*m/z* 411.18), e. $Cu(I)(H_2O)(CH_3OPiv)_3]^+$ (*m/z* 429.19), f. $[Cu(I)OPiv(1)(2)]^+$ (*m/z* 450.14)

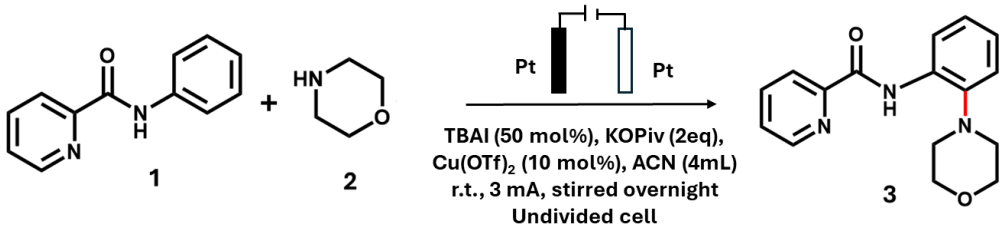

Fig. S15. Bulk reaction of C-H amination of *N*-phenylpicolinamide with morpholine in an undivided cell utilizing 10 mol% of $Cu(OTf)_2$ as the source of catalyst with the following specifications: **1** (0.2 mmol), **2** (4.0 equiv), $Cu(OTf)_2$ (10mol %), KOPiv (2.0 equiv), n-Bu_4NI (50 mol %), and CH_3CN (4mL), in an undivided cell with two platinum electrodes (each 1.5 ×1.0 cm^2), 27 °C, 3.0 mA, stirred for 24 h^1.

Table S1: Intensities of *N*-phenylpicolinamide (limiting reagent), intermediates, and product peaks of C-H for bulk synthesis utilizing $Cu(OTf)_2$ as the Cu catalyst

Time	Limiting Reagent ($I_{L.R.}$)	Intermediates (I_{int})					Product (I_P)				Conversion Ratio	Intensity Ratio
min	*m/z* 199	*m/z* 261	*m/z* 362	*m/z* 347	*m/z* 448	*m/z* 346	*m/z* 322	*m/z* 306	*m/z* 284	$I_{SUM} = \Sigma(I_P + I_{int})$	$(I_{SUM}/(I_{SUM}+I_{L.R.}))*100$	$(I_{SUM}/I_{L.R.})*100$
2	4.17E+06	8.21E+04	4.61E+04	2.10E+04	8.46E+03	5.59E+03	1.18E+04	2.70E+04	9.48E+04	2.97E+05	6.65E+00	7.12E+00
5	4.12E+04	1.06E+03	2.45E+03	6.79E+02	3.22E+02	3.52E+02	2.59E+02	1.53E+03	1.00E+03	7.65E+03	1.57E+01	1.86E+01
15	3.54E+06	2.27E+06	5.80E+04	5.95E+04	3.17E+04	1.69E+04	1.65E+04	4.01E+04	3.30E+04	2.53E+06	4.16E+01	7.13E+01
hr	-	-	-	-	-	-	-	-	-	-	-	-
6	7.58E+06	2.12E+06	1.98E+04	5.31E+05	4.58E+03	1.24E+05	4.40E+06	9.27E+06	5.86E+06	2.23E+07	7.47E+01	2.95E+02
24	4.89E+06	6.34E+05	8.21E+03	1.78E+05	3.05E+04	4.46E+04	2.89E+06	4.76E+06	8.05E+06	1.66E+07	7.72E+01	3.39E+02

The conversion ratio % of C-N coupled product and intermediates from the limiting reagent was calculated using Equation S1, an example below at 15 minutes, showing a conversion ratio % of 4.16E+01

Equation S1: Conversion Ratio $= (\Sigma I_{SUM}/(\Sigma I_{SUM}+I_{L.R..}))*100$ = (2.53E+06/(2.53E+06 + 3.54E+06) = 4.16E+01

Where, $I_{SUM} = \Sigma(I_P + I_{int})$

The ratio of peak intensities of C-N coupled product to the limiting reagent was calculated using Equation S2, an example below at 15 minutes, showing an intensity ratio of 1.43E+01

Equation S2: Intensity Ratio $= (\Sigma I_{SUM}/(\Sigma I_{L.R.}))*100$ = (2.53E+06/3.54E+06) = 7.13E+01

Table S2: Intensities of *N*-phenylpicolinamide (limiting reagent), intermediates, and product peaks of C-H for online synthesis utilizing in situ electrolytically generated Cu catalyst in nanoelectrospray

Time	Limiting Reagent ($I_{L.R.}$)	Intermediates (I_{int})					Product (I_P)				Conversion Ratio	Intensity Ratio
min	*m/z* 199	*m/z* 261	*m/z* 362	*m/z* 347	*m/z* 448	*m/z* 346	*m/z* 322	*m/z* 306	*m/z* 284	$I_{SUM} = \Sigma(I_P + I_{int})$	$(I_{SUM}/(I_{SUM}+I_{L.R.}))*100$	$(I_{SUM}/I_{L.R.})*100$
2	1.13E+06	7.02E+05	4.58E+04	1.86E+06	2.24E+04	4.66E+05	1.03E+04	5.37E+04	0.00E+00	3.16E+06	7.37E+01	2.80E+02
5	4.86E+05	8.86E+05	3.16E+05	1.14E+06	1.46E+06	4.78E+05	1.55E+04	2.03E+05	0.00E+00	4.50E+06	9.02E+01	9.26E+02
10	7.82E+03	3.44E+05	1.40E+05	7.36E+05	9.31E+03	3.90E+05	1.54E+04	9.91E+04	0.00E+00	1.73E+06	9.96E+01	2.22E+04
15	5.71E+03	2.83E+03	1.24E+05	7.50E+05	1.33E+04	3.08E+05	1.54E+04	6.48E+04	0.00E+00	1.28E+06	9.96E+01	2.24E+04

Apparent Acceleration Factor (AAF) was calculated using Equation S3, by comparing the intensity ratio of online synthesis versus bulk synthesis, at a time point of 15 minutes.

Equation S3: $AAF = Intensity\ Ratio_{\ in\ situ\ Cu\ catalyst} / Intensity\ Ratio_{\ traditional\ Cu\ catalyst}$

= 2.24E+04/ 7.13E+01 = 3.14E+02

A key feature repeatedly demonstrated in microdroplet and nanoelectrospray studies is that reactions can exhibit apparent rate enhancements relative to bulk solution due to the unique physicochemical environment of confined droplets. These effects have been attributed to factors such as high surface-to-volume ratios, rapid solvent evaporation, and enrichment of reactive species at or near the droplet interface, all of which can collectively alter effective reaction rates.

For this reason, comparisons of product formation under nominally similar starting conditions have commonly been used in the literature as a practical way to illustrate microdroplet-induced acceleration effects, particularly when direct extraction of intrinsic rate constants is challenging due to the fundamentally different reaction environments.

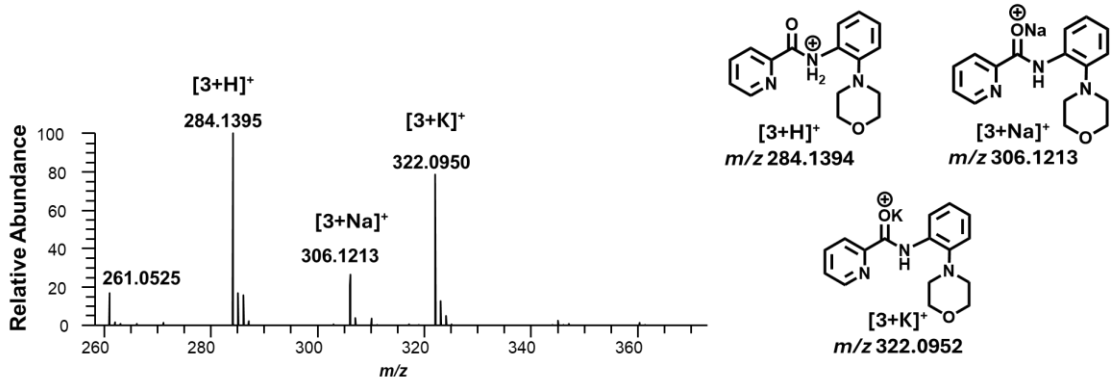

Fig. S16. High resolution MS (HRMS) of the product peaks from bulk synthesis of C-H amination of *N*-phenylpicolinamide with morpholine after 24 hrs identified at *m/z* 284.1394 $[3+H]^+$, *m/z* 306.1213 $[3+Na]^+$, *m/z* 322.0952 $[3+K]^+$

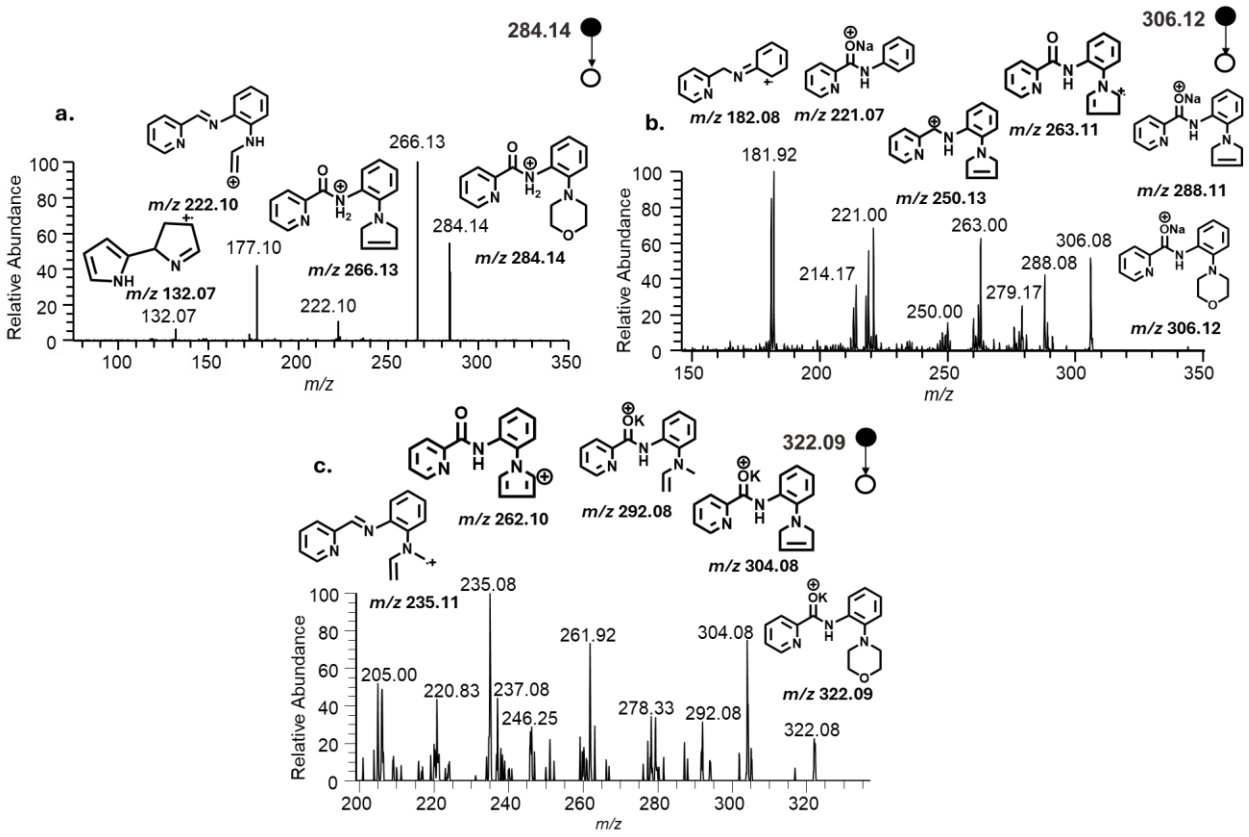

Fig. S17. Tandem of product peaks from bulk synthesis of C-H amination of *N*-phenylpicolinamide with morpholine after 24 hrs: a. FT-MS/MS of $[3+H]^+$ (*m/z* 284.14), b. IT-MS/MS of $[3+Na]^+$ (*m/z* 306.12), d. IT-MS/MS of $[3+K]^+$ (*m/z* 322.09)

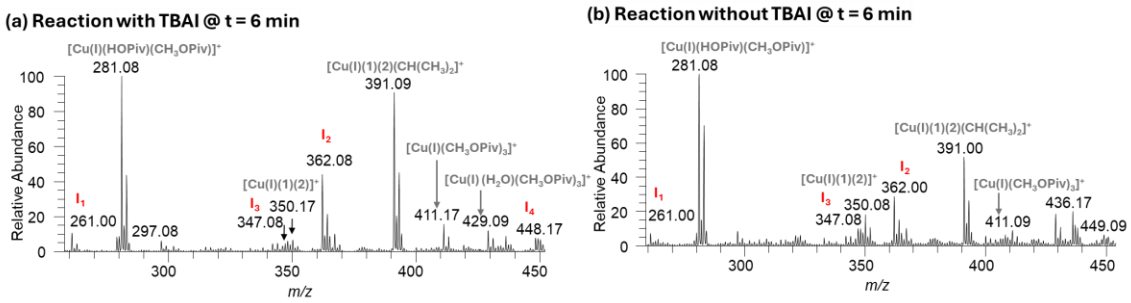

Fig. S18 Online C-H amination of *N*-phenylpicolinamide with morpholine, reaction captured at 6 minutes when conducted in: a) the presence of TBAI results in the observation of intermediates **I_1** (*m/z* 261.00), **I_2** (*m/z* 362.00), and **I_3** (*m/z* 347.08) and **I_4** (*m/z* 448.17) b) the absence of TBAI results in the observation of **I_1** (*m/z* 261.00), **I_2** (*m/z* 362.00), and **I_3** (*m/z* 347.08) but no **I_4** (*m/z* 448.17). This shows the contribution of the oxidation of iodine radical, contributing to the generation of the high-valent Cu(III)-intermediate **I_4**

S6. Mild and efficient Cu-catalyzed online electrochemical N-N homocoupling of *o*-phenylenediamine to form N-substituted benzotriazole

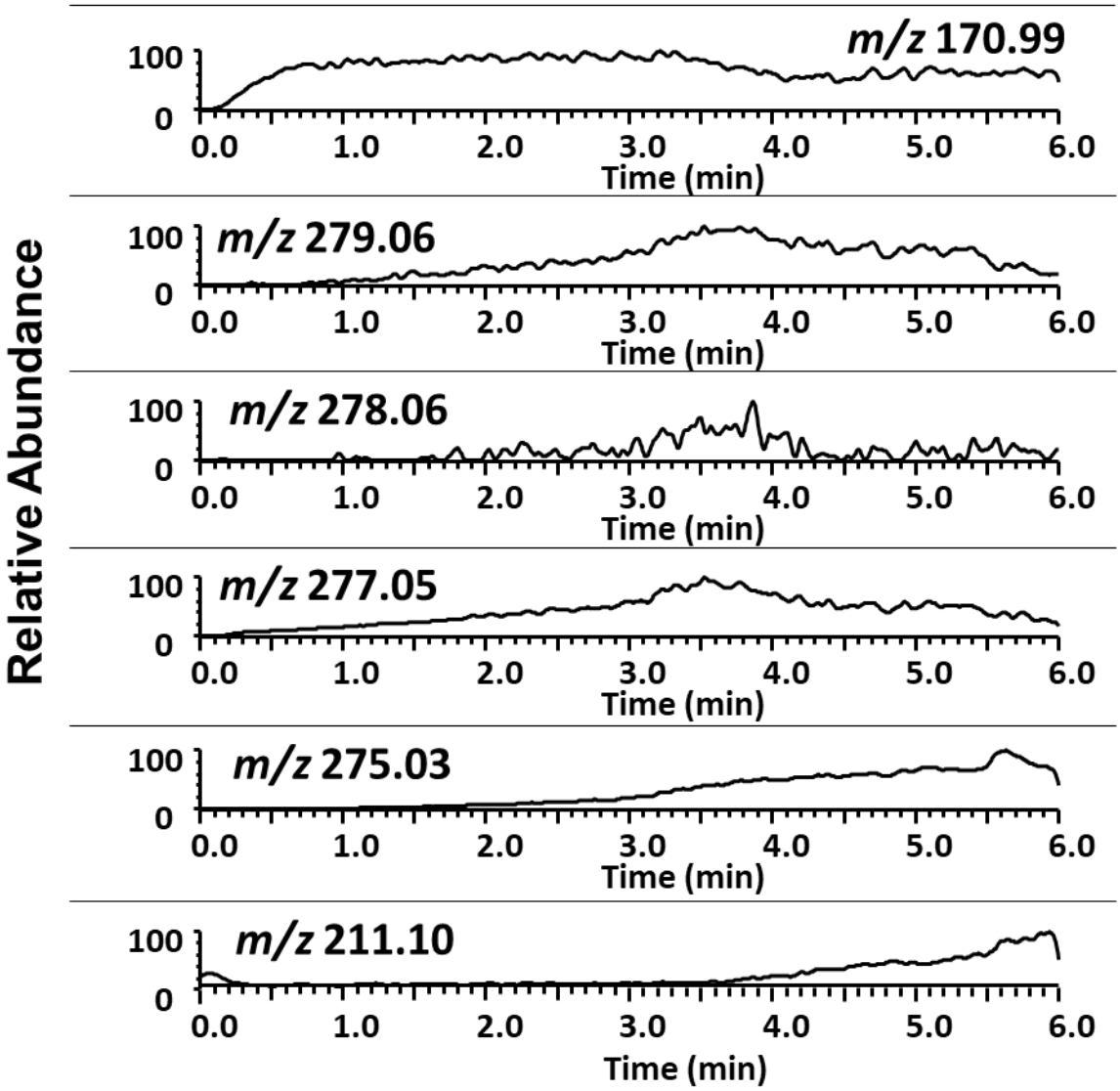

Fig. S19. Extracted ion chromatogram (XIC) of Cu-mediated intermediates and product of mild and efficient Cu-catalyzed online electrochemical N-N homocoupling to form substituted benzotriazole from *o*-phenylenediamine. XIC shows that initial intermediates at *m/z* 170.99 forms within a few seconds of voltage application and decreases after 4 minutes. Intermediates at *m/z* 279.06, *m/z* 278.06, and *m/z* 277.05, form at 2 minutes and start to decrease at 4 minutes. At 4 minutes, the concentration of the later intermediate at *m/z* 275.03, and of product *m/z* 211.10, shows increasing concentration over time. The reaction was stopped at 6 minutes to ensure reaction monitoring with a stable Total Ion Chromatogram (TIC).

* the initial signal intensity seen in XIC of *m/z* 211.10 is attributed to the background contamination signal of comparable mass-to-charge ratio.

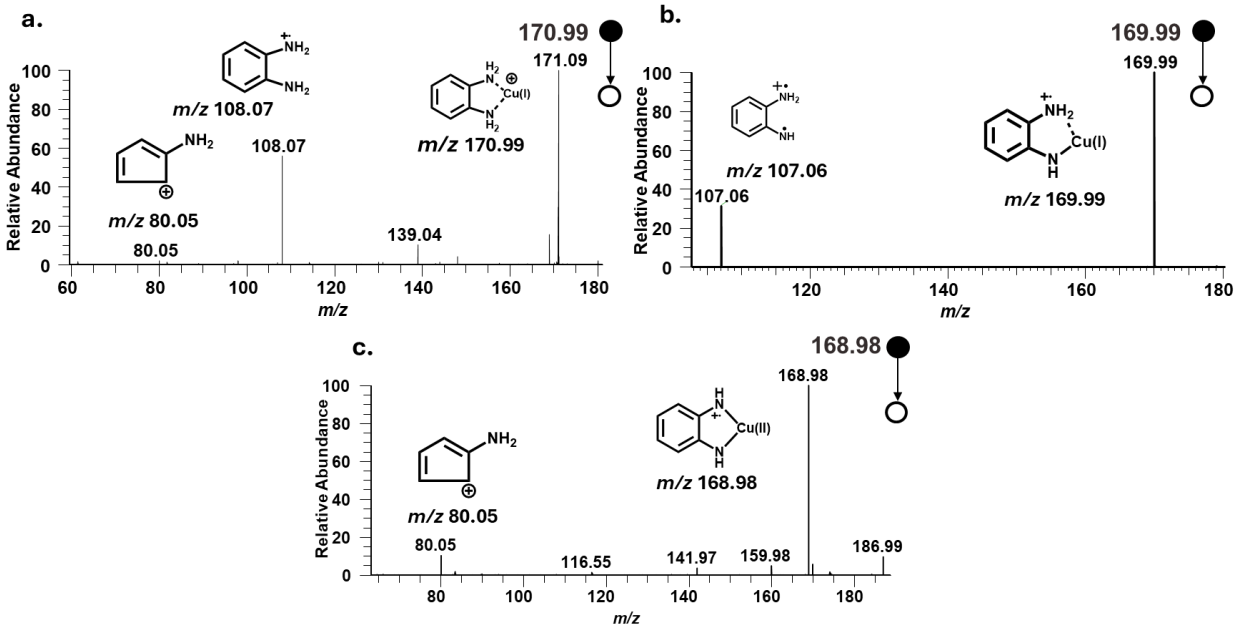

Fig. S20. Tandem of Cu-mediated radical intermediates from mild and efficient Cu-catalyzed online electrochemical N-N homocoupling of *o*-phenylenediamine to form N-substituted benzotriazole: a. $\mathbf{II_1}$ (*m/z* 170.99), b. $[Cu(I)(4\text{-}H)]^{\cdot+}$ (*m/z* 169.99), c. $[Cu(II)(4\text{-}2H)]^{\cdot+}$ (*m/z* 168.98)

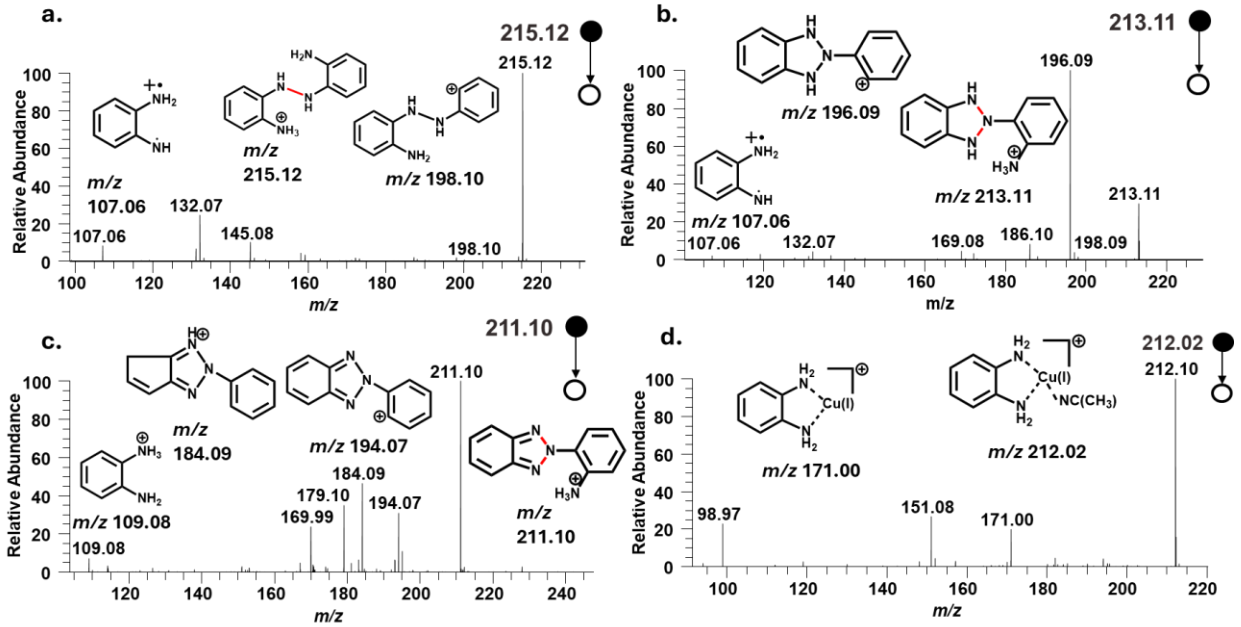

Fig. S21. Tandem of N-N dimerized, cyclized intermediate and product from mild and efficient Cu-catalyzed online electrochemical N-N homocoupling of *o*-phenylenediamine to form N-substituted benzotriazole: a. N-N dimerized intermediate $[\mathbf{II_5}\text{-}Cu(I)+H]^+$ (*m/z* 215.12), b. Cyclized intermediate $\mathbf{II_8}$ (*m/z* 213.11), c. Product **5** (*m/z* 211.10) d. Cu(I)-adducted peak of $[Cu(I)(OPD)(ACN)]^+$ (*m/z* 212.02)

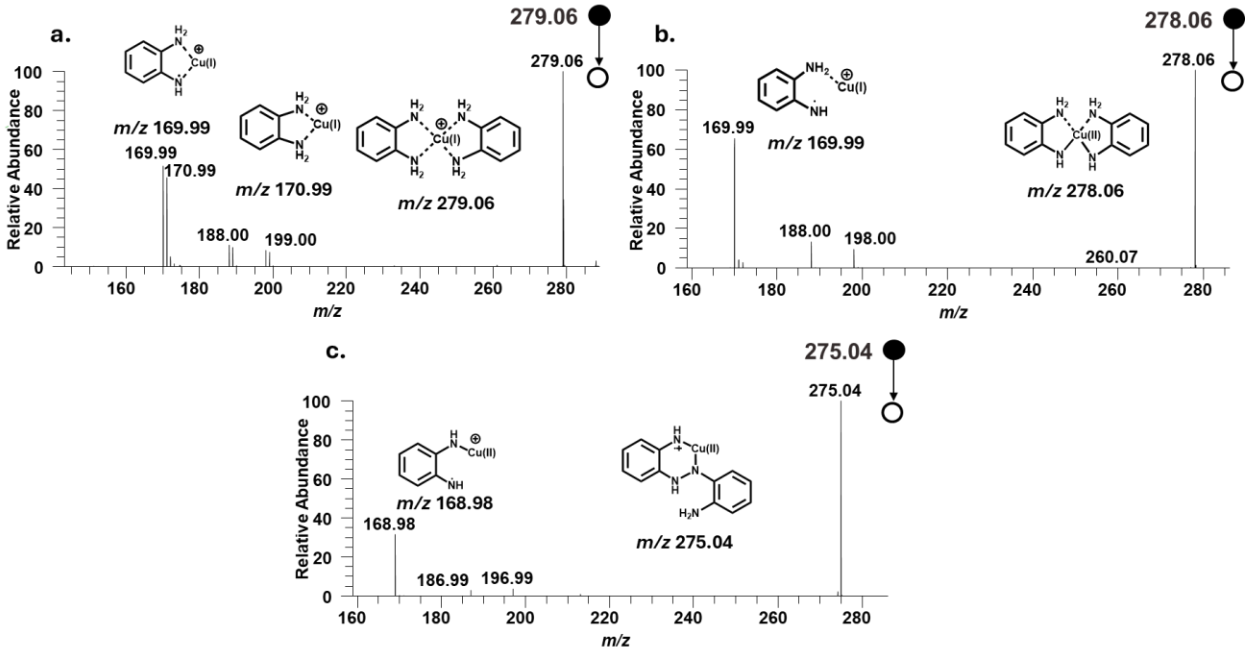

Fig. S22. Tandem of Cu-mediated radical intermediates from mild and efficient Cu-catalyzed online electrochemical N-N homocoupling of *o*-phenylenediamine to form N-substituted benzotriazole: a. **II_2** (at *m/z* 279.06), b. **II_3** (at *m/z* 278.06), c. **II_7** (at *m/z* 275.04)

Table S3: Cu-intermediates and product of N-N coupling of *o*-phenylenediamine detected by nanoESI-MS

Intermediate/Product	Theoretical *m/z*	Observed *m/z*	Δ ppm
II_1	170.9978	170.9977	-0.58
II_2	279.0665	279.0659	-2.15
II_3	278.0587	278.0582	-1.80
II_5	277.0509	277.0501	-2.89
II_7	275.0358	275.0353	-1.82
5	211.0978	211.0975	-1.42

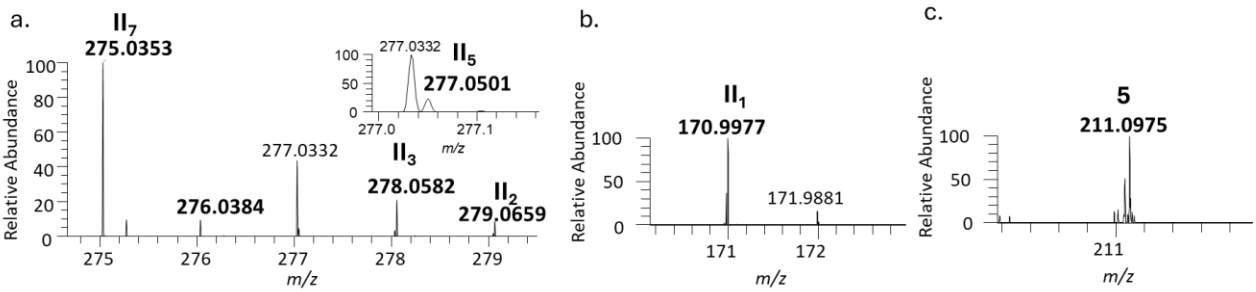

Fig. S23. HRMS of intermediates and products of N-N coupling of *o*-phenylenediamine: a. Cu-intermediates **II_2** (*m/z* 279.0659), **II_3**(*m/z* 278.0582), **II_5** (*m/z* 277.0501), and **II_7** (*m/z* 275.0353), b. Cu-intermediate **II_1** (*m/z* 170.9977), c. 2-(2H-Benzotriazol-2-yl)benzenamine (**5**) (*m/z* 211.0975)

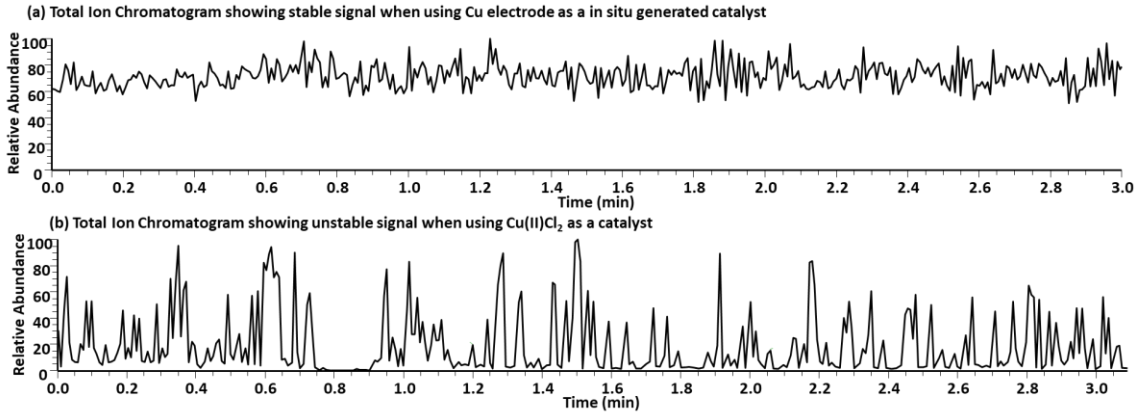

Fig. S24. Total Ion Chromatogram over 3 minutes showing (a) stable total ion intensity when Cu electrode is used as an in situ source of catalyst in nanoESI, versus (b) unstable total ion intensity when Cu(II)Cl_2 is used as a catalyst, as salt suppresses signal and interferes with MS analysis.

Table S4: Intensities of starting material, intermediates, and product peaks of N-N homocoupling of OPD tracked for 3 minutes, catalyzed by Cu salt catalyst in the nanoESI based online microreactor

Time	Starting material ($I_{S.M.}$)	Product (I_P)	Intermediates (I_{int})							I_{SUM}	Conversion Ratio	Intensity Ratio
min	*m/z* 109	*m/z* 211	*m/z* 213	*m/z* 215	*m/z* 275	*m/z* 277	*m/z* 278	*m/z* 279	*m/z* 170.99	$= \Sigma(I_P + I_{int})$	$(I_{SUM}/(I_{SUM}+I_{S.M.}))*100$	$(I_{SUM}/I_{S.M.})*100$
0.5	1.75E+06	2.41E+04	2.98E+03	3.51E+03	1.27E+05	3.58E+02	3.37E+02	1.03E+02	5.48E+02	1.35E+05	7.15E+00	7.70E+00
1	2.18E+06	1.80E+04	3.68E+03	4.74E+03	1.88E+05	2.92E+02	1.52E+02	3.39E+02	1.57E+03	1.99E+05	8.36E+00	9.12E+00
2	2.00E+06	2.77E+04	6.50E+03	2.94E+03	1.83E+05	9.86E+02	4.45E+02	2.65E+02	8.62E+02	1.95E+05	8.88E+00	9.75E+00
3	2.47E+06	2.64E+04	8.28E+03	3.83E+03	2.76E+05	8.63E+02	5.67E+01	1.12E+03	1.42E+03	2.92E+05	1.06E+01	1.18E+01

Table S5: Intensities of starting material, intermediates, and product peaks of N-N homocoupling of OPD tracked for 3 minutes, catalyzed by in situ electrolytically generated Cu catalyst in the nanoESI-based online microreactor

Time	Starting material ($I_{S.M.}$)	Product (I_P)	Intermediates (I_{int})							$I_{SUM} = \Sigma(I_P + I_{int})$	Conversion Ratio $(I_{SUM}/(I_{SUM}+I_{S.M.}))*100$	Intensity Ratio $(I_{SUM}/I_{S.M.})*100$
min	*m/z* 109	*m/z* 211	*m/z* 213	*m/z* 215	*m/z* 275	*m/z* 277	*m/z* 278	*m/z* 279	*m/z* 170.99			
0.5	1.09E+06	3.70E+03	0.00E+00	1.18E+05	2.88E+04	5.88E+03	1.85E+04	2.09E+04	2.17E+05	4.09E+05	2.73E+01	3.75E+01
1	1.16E+06	3.61E+03	5.45E+03	1.13E+05	4.39E+04	1.01E+04	3.33E+04	1.64E+04	3.03E+05	5.25E+05	3.12E+01	4.53E+01
2	1.21E+06	4.75E+03	5.92E+03	1.17E+05	2.02E+05	2.27E+04	4.94E+04	1.67E+04	3.48E+05	7.62E+05	3.86E+01	6.30E+01
3	1.19E+06	6.15E+03	6.18E+03	1.16E+06	4.86E+05	3.74E+04	5.52E+04	1.20E+04	3.48E+05	2.10E+06	6.39E+01	1.77E+02

Utilizing Equations S1-S3, the conversion ratio % achieved at 3 minutes utilizing the in situ electrolytically generated Cu cations is 6.39E+01 versus a conversion ratio % of 1.06E+01 catalyzed by Cu salt in the online microreactor.

The AAF calculated utilizing the intensity ratio is shown below:

$$AAF = \text{Intensity Ratio}_{\text{in situ Cu catalyst}} / \text{Intensity Ratio}_{\text{traditional Cu catalyst}} = 1.77E+02 / 1.18E+01 = 1.50E+01$$

Showing a ~10-fold acceleration in the reaction progression when catalyzed by in situ electrolytically generated Cu cations versus Cu salt.

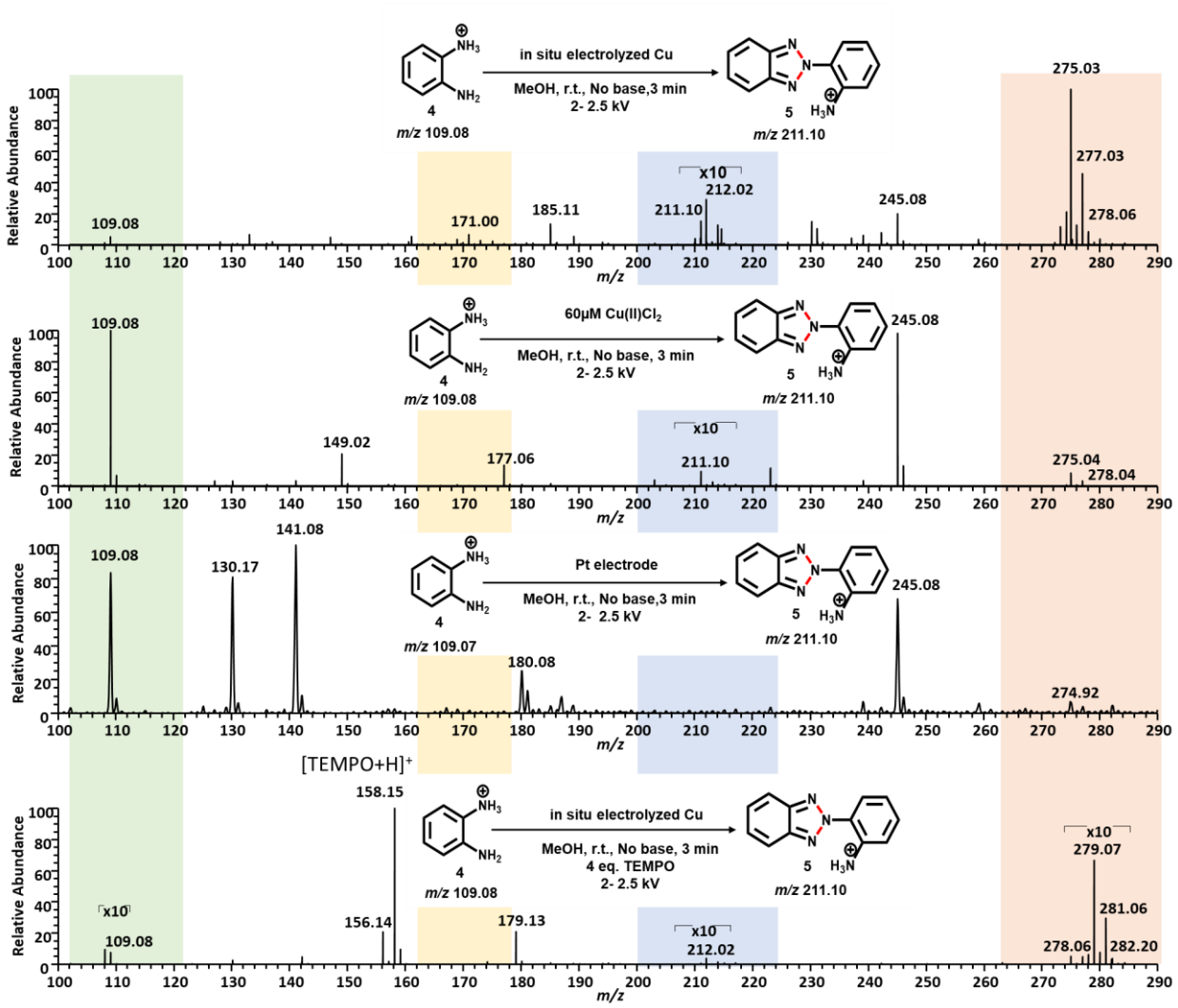

Fig. S25. Comparison of N-N homocoupling of *o*-phenylenediamine to form N-substituted benzotriazole to observe the reaction progression under different catalytic conditions: (a) in situ electrolyzed Cu in the TM electrochemical microreactor, (b) $Cu(II)Cl_2$ salt in the nanoESI emitter, Cu-salt catalyzed spectrum generated unstable signal; no radical, Cu-mediated intermediates, or product was observed in comparatively lower abundance compared to in situ electrolyzed Cu cations (where the radical, Cu-mediated intermediates were observed within 1 minute and product was observed within 3 minutes of reaction initiation) (c) control showing *o*-phenylenediamine solution sprayed with Pt as the electrode in the nanoESI emitter, no observed intermediates/product peaks (d) Radical trapping with 4 equivalents of 2,2,6,6-Tetramethylpiperidin-1-yl)oxyl (TEMPO), at 3 minutes, with same reaction conditions, generates no Cu(I)-mediated amine radical intermediates, no major product **5** (at *m/z* 211.10).
[Starting material, **4** at *m/z* 109.08 (green); Cu(I)-intermediates with single OPD molecule, at *m/z* 171.00, *m/z* 168.98 (yellow); product peak, **5** at *m/z* 211.10 (blue); Cu(I)-redox active amine radical intermediate at *m/z* 275.03 (orange)]

S7. Mild and efficient Cu-catalyzed online electrochemical dehydrogenative intramolecular N-N coupling of anthranilamide to form 3-indazolinone

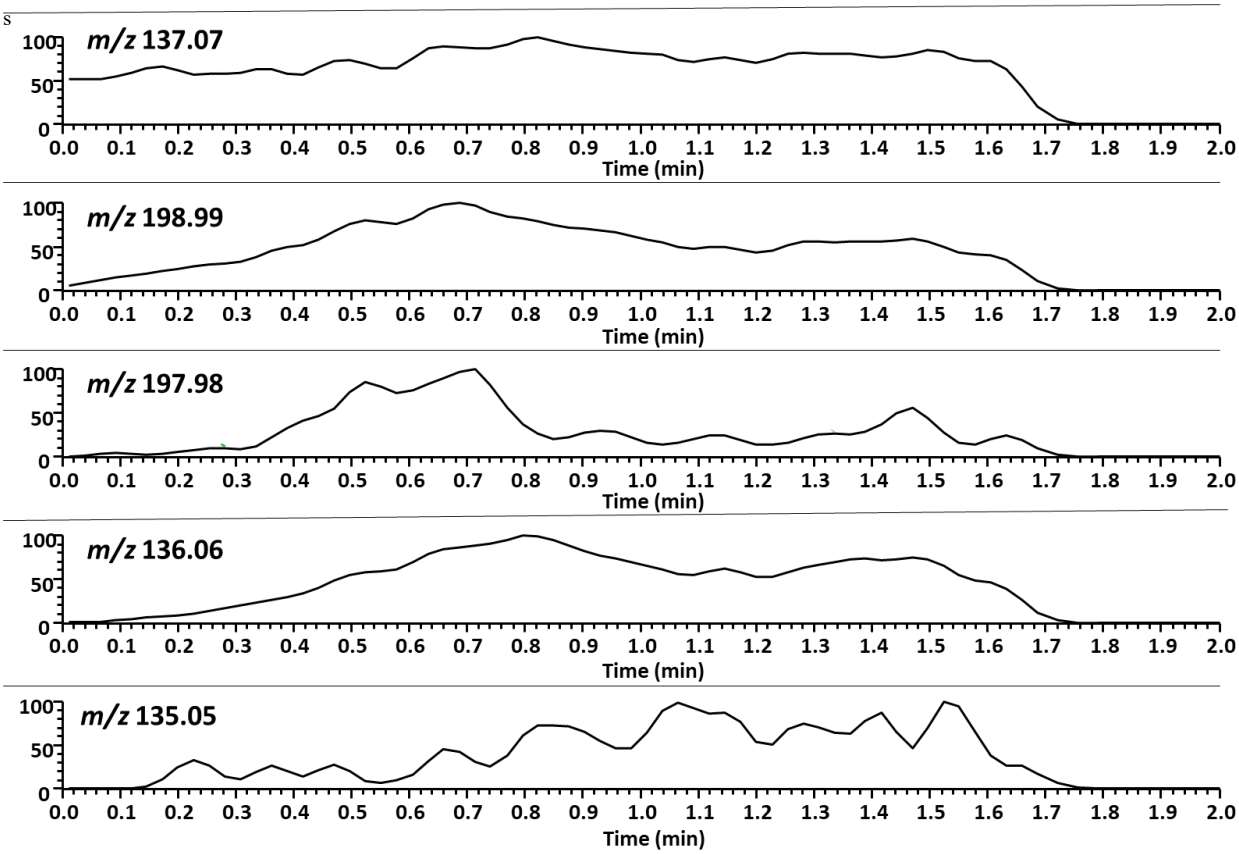

Fig. S26. Extracted ion chromatogram (XIC) of starting material, intermediates, and products from mild and efficient copper-catalyzed online electrochemical dehydrogenative intramolecular N-N coupling of anthranilamide to form 3-indazolinone. The XIC of the starting material at *m/z* 137.07 remains constant over the period of 2 minutes. The radical intermediate and the Cu(I)-intermediate at *m/z* 136.06 and *m/z* 198.99 respectively, form at 0.2 minutes. The intensity of Cu(I)-amine radical intermediate at *m/z* 197.98 could be traced to form around 0.3 minutes. The product intensity at *m/z* 135.05 indicates it is slowly forming over time, with increasing intensity over the reaction time. The reaction was stopped at 1.7 minutes to ensure reaction monitoring with a stable Total Ion Chromatogram (TIC).

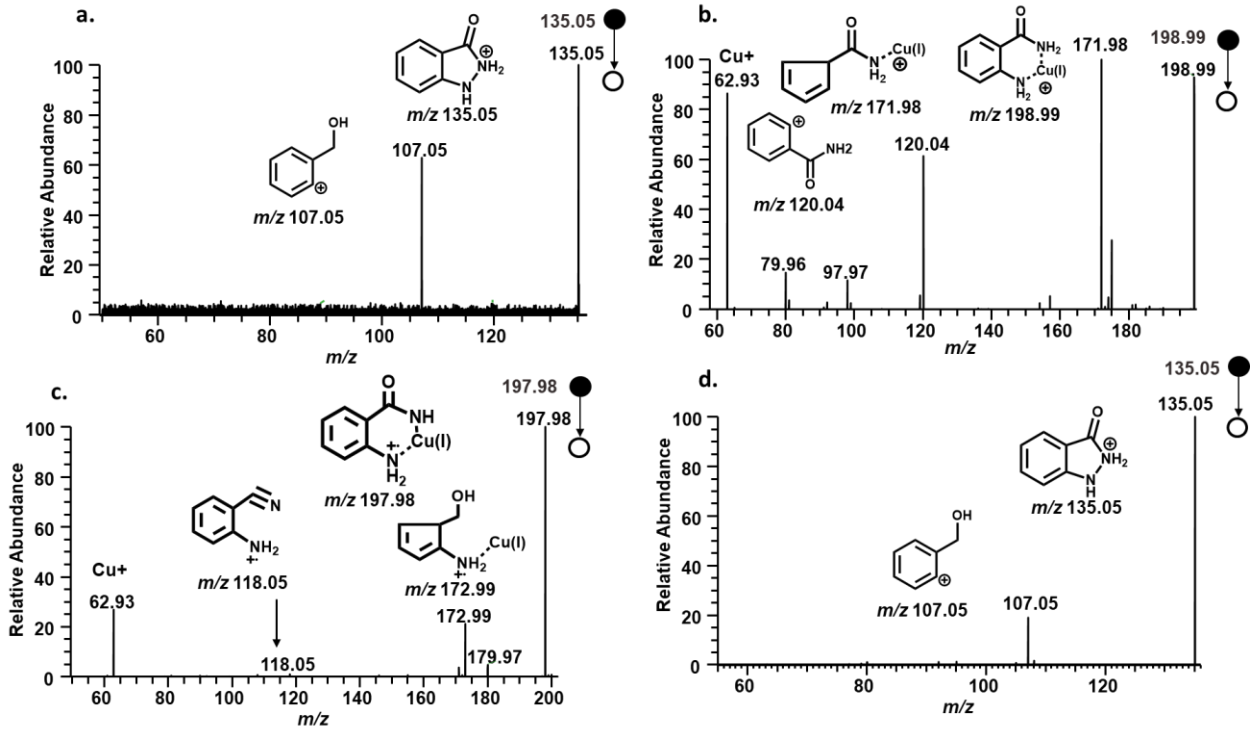

Fig. S27. Tandem of product and Cu-mediated intermediate from mild and efficient Cu-catalyzed online electrochemical dehydrogenative intramolecular N-N coupling of anthranilamide to form 3-indazolinone: a. Product **7** (at *m/z* 135.05), b. Cu(I)-intermediate **III$_2$** (at *m/z* 198.99), c. Cu(I)-amine radical intermediate **III$_4$** (at m/z 197.98). d. Tandem of purchased reference compound 3-Indazolinone used as standard to confirm tandem MS of identified product **7**

Table S6: Intermediates and product of dehydrogenative intramolecular N-N coupling of anthranilamide detected by nanoESI-MS

Intermediate/ Product	**Theoretical *m/z***	**Observed *m/z***	**Δ ppm**
III_1	136.0631	136.0631	0.00
III_2	198.9927	198.9926	-0.50
III_4	197.9849	197.9848	-0.51
7	135.0553	135.0550	-2.22

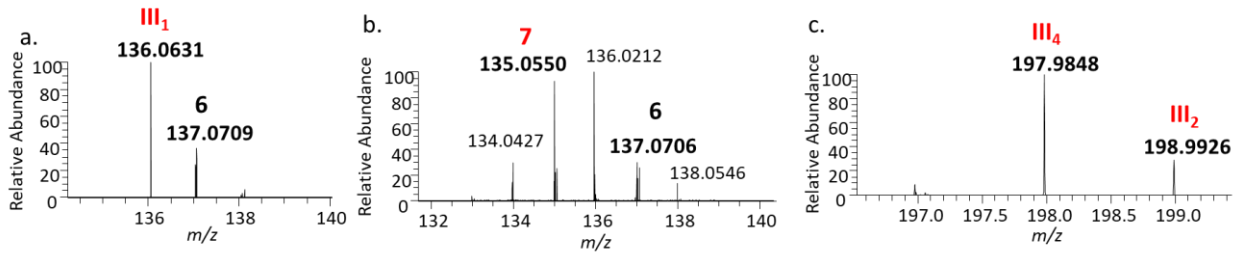

Fig S28. HRMS of intermediates and products of dehydrogenative intramolecular N-N coupling of anthranilamide: a. Radical intermediate **III_1** (*m/z* 136.0631), b. Product 3-indazolinone **7** (*m/z* 135.0550), c. Cu(I)-intermediate **III_2** (*m/z* 198.9926) and Cu(I)-amine radical intermediate **III_4** (at m/z 197.9848)

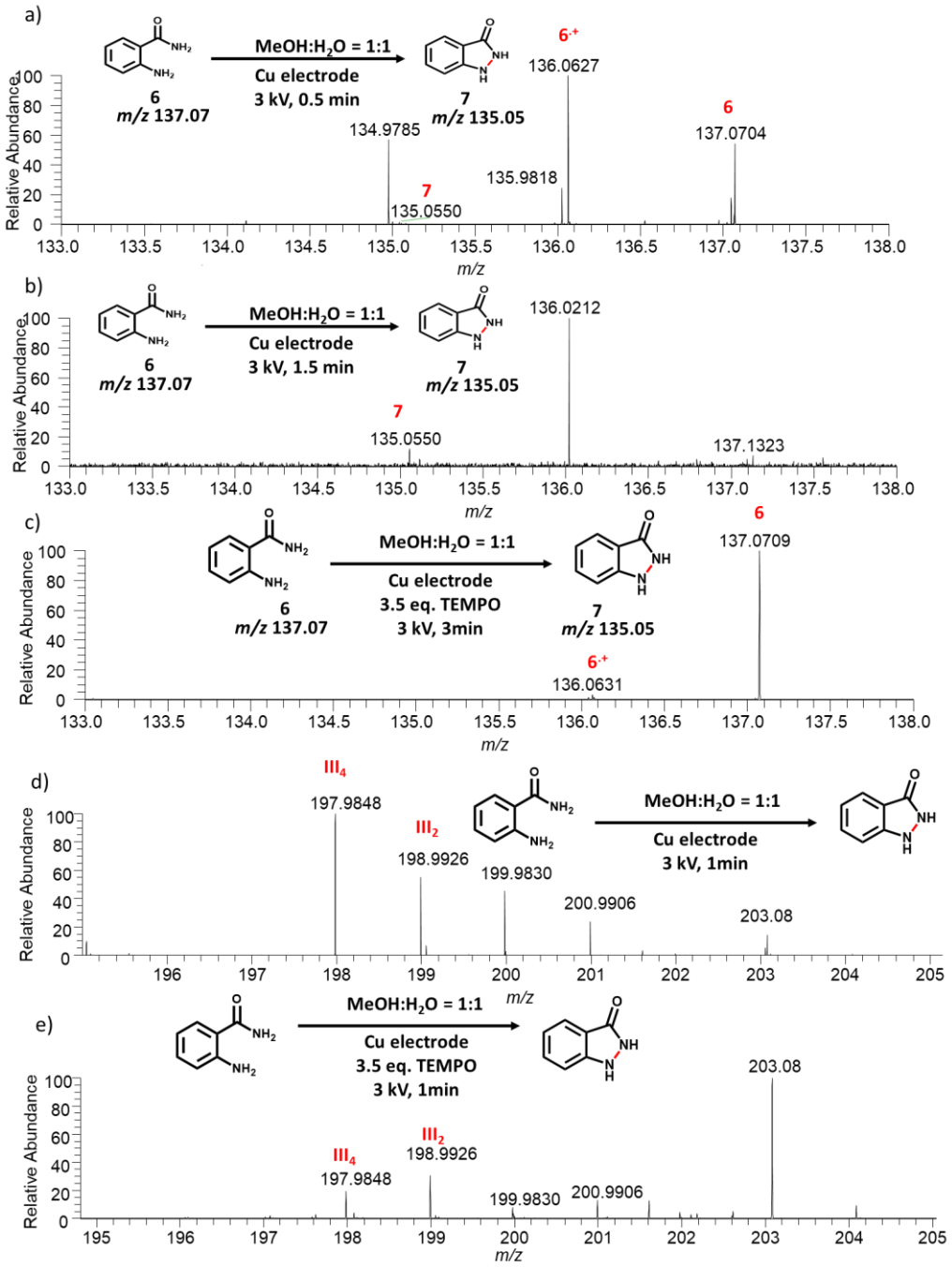

Fig. S29. Mechanistic insight into Cu-catalyzed online electrochemical dehydrogenative intramolecular N-N coupling of anthranilamide with HR-MS under different conditions. a) 3kV application with Cu electrode for 0.5 min generates the radical intermediate **6**$^{\cdot+}$ *m/z* 136.0627 from **6** *m/z* 137.0704, which, after, b) 1.5 minutes, generates the N-N coupled product **7** *m/z* 135.0550. Upon radical trapping with 3.5 equivalents of 2,2,6,6-Tetramethylpiperidin-1-yl)oxyl (TEMPO), c) the spectrum shows observation of very little radical intermediate **6**$^{\cdot+}$ *m/z* 136.0631 and no product with starting material **6** *m/z* 137.0709 as the major peak

even after 3 min. This indicates that Cu-mediated radical-mechanism is the key pathway driving reaction progression. d) Cu(I)-intermediate **III$_2$** *m/z* 198.9926 and Cu(I)-amine radical intermediates **III$_4$** *m/z* 197.9848 formed after 0.8 – 1 min upon application of 3kV with Cu electrode. e) Upon radical trapping with 3.5eq. of TEMPO, the abundance of Cu(I)-intermediate **III$_2$** *m/z* 198.9926 and Cu(I)-amine radical intermediates **III$_4$** *m/z* 197.9848 decreases significantly indicating the involvement of Cu-mediated radical pathway.

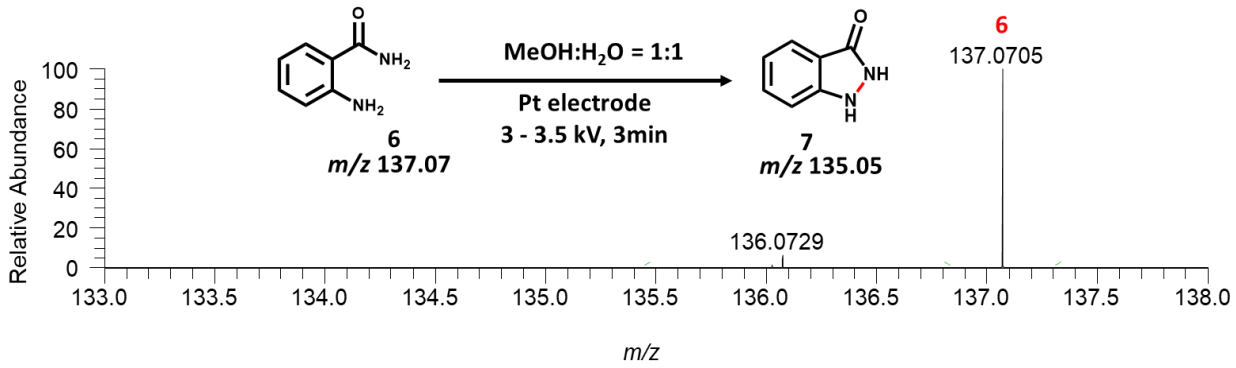

Fig. S30. Upon replacing the Cu electrode with an inert Pt electrode and applying voltage for 3 min, no radical intermediate or product peaks are observed with the starting material *m/z* 137.0705 dominating the spectrum. This indicates the importance of the in situ-generated Cu catalyst for initiating SET and the involvement of Cu oxidative cycle, generating the key Cu-complex and radical intermediates, and achieving N-N coupling.

S8. Scale-up of in situ Cu-catalyzed electrochemical C–H amination in an electrochemical cell

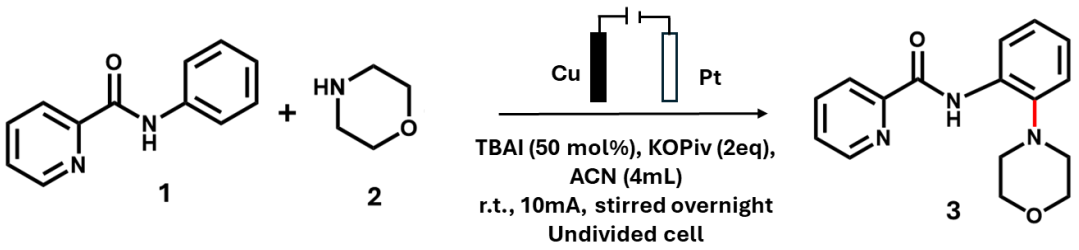

Fig. S31. Scale-up of in situ Cu-catalyzed electrochemical C–H amination of *N*-phenylpicolinamide with morpholine in an electrochemical cell

To demonstrate the feasibility of transferring the in situ generated copper electrocatalyst system from nanoelectrospray to conventional bulk electrosynthesis, the scale-up of C-H amination of *N*-phenylpicolinamide **1** (0.4mmol) with morpholine **2** (4 eq.) was performed with potassium pivalate (KOPiv, 2 equiv), and tetra-n-butylammonium iodide (TBAI, 50 mol%) in 4 ml ACN solvent at room temperature in an undivided cell (40mm x 97.5 mm) with Cu anode (8 mm x 6 mm x 2 mm) and Pt foil cathode (8 mm x 6 mm x 1.25 mm). A constant current of 10mA was applied to the reaction mixture, being stirred at room temperature overnight. The reaction mixture was concentrated in vacuum, followed by extraction with EtOAc and saturated ammonium chloride (3 × 10 mL). The crude product was purified by column chromatography on silica gel using EtOAc/Hexane. The product was characterized by ^{1}H NMR, ^{13}C NMR, and HRMS.

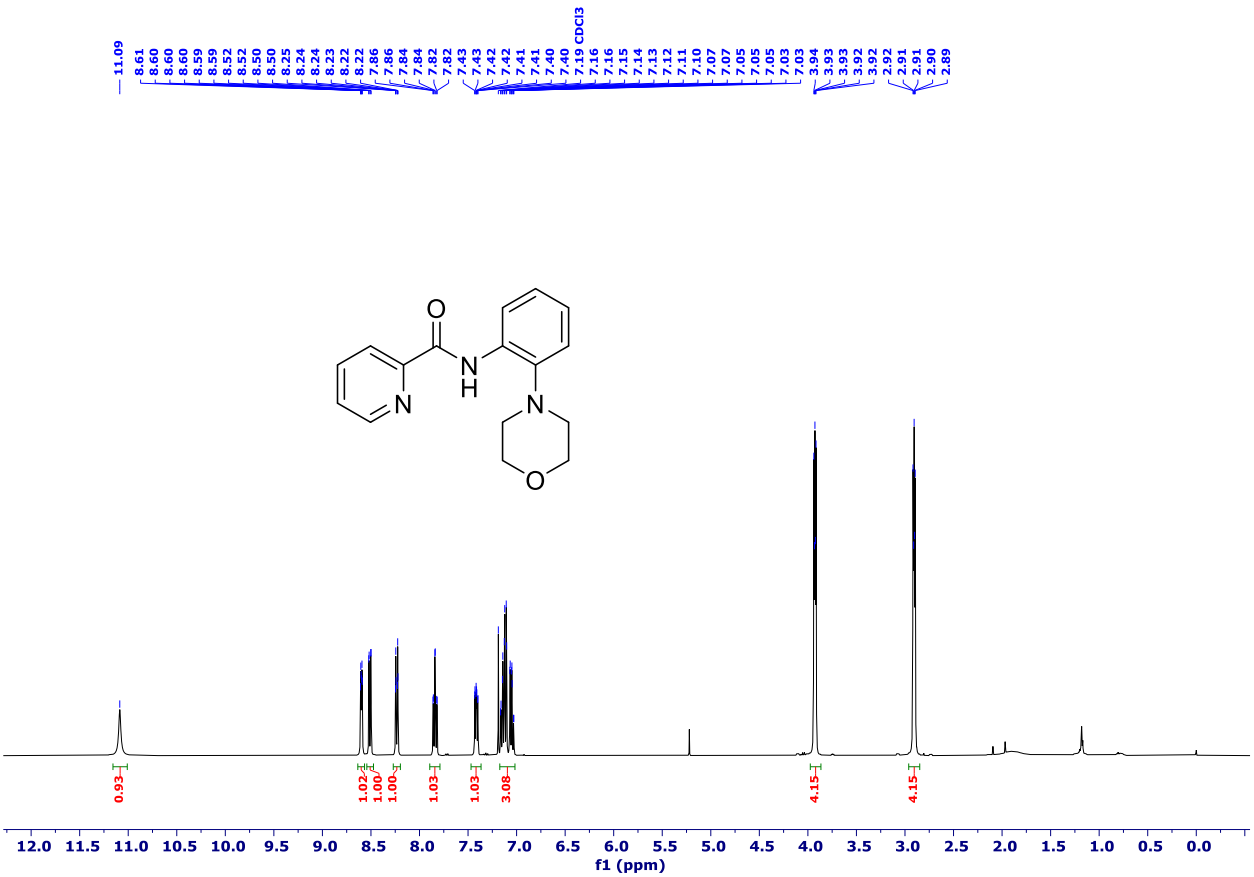

Fig. S32: ^{1}H NMR of **3** ($CDCl_3$, 400 MHz) after purification by silica gel flash chromatography

^{1}H NMR (400 MHz, $CDCl_3$) δ 11.09 (s, 1H), 8.64 – 8.57 (m, 1H), 8.51 (dd, *J* = 8.1, 1.5 Hz, 1H), 8.27 – 8.20 (m, 1H), 7.84 (td, *J* = 7.7, 1.7 Hz, 1H), 7.47 – 7.37 (m, *J* = 7.7, 4.7, 1.2 Hz, 1H), 7.17 – 7.02 (m, 3H), 3.98 – 3.87 (m, 4H), 2.96 – 2.85 (m, 4H).

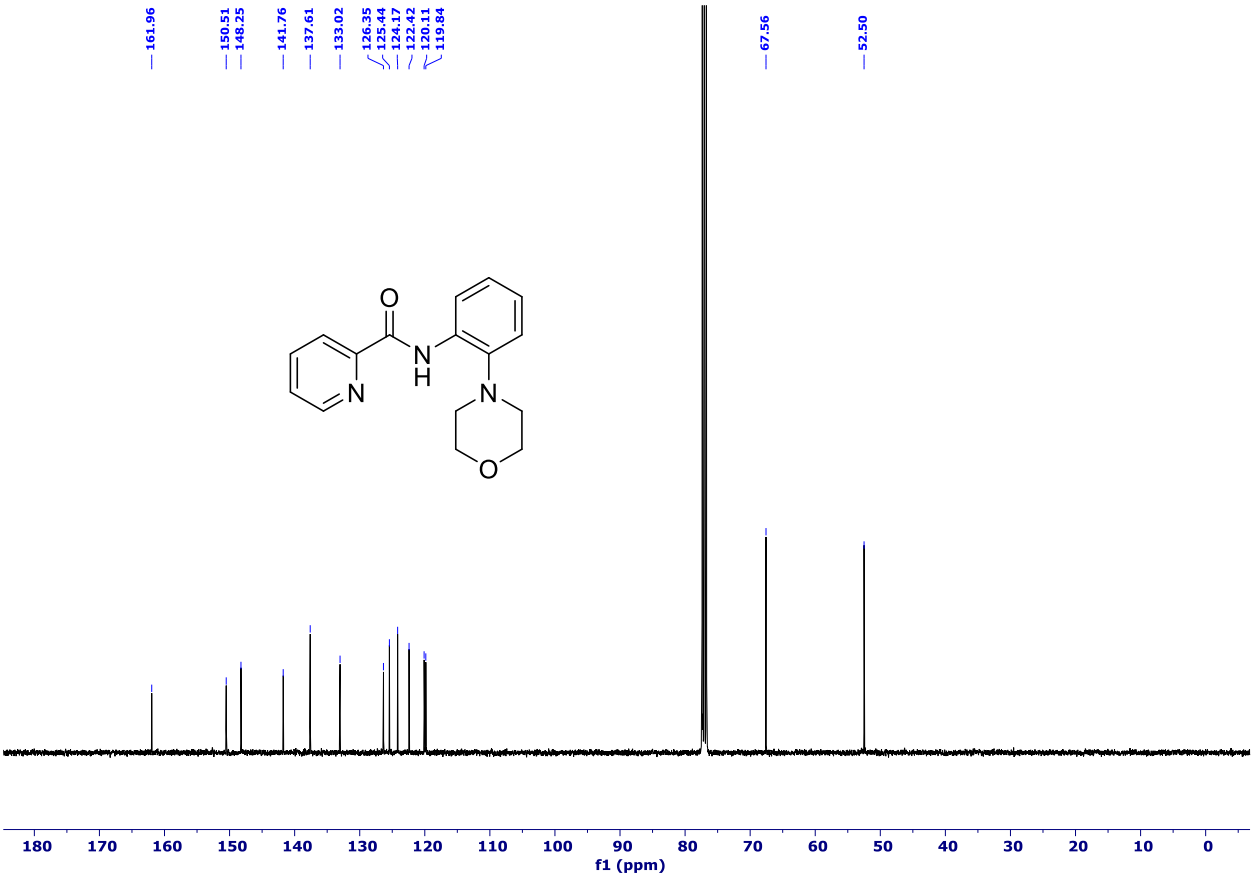

Fig. S33: ^{13}C NMR of **3** ($CDCl_3$, 101 MHz) after purification by silica gel flash chromatography

^{13}C NMR (101 MHz, CDCl3) δ 161.96, 150.51, 148.25, 141.76, 137.61, 133.02, 126.35, 125.44, 124.17, 122.42, 120.11, 119.84, 67.56, 52.50.

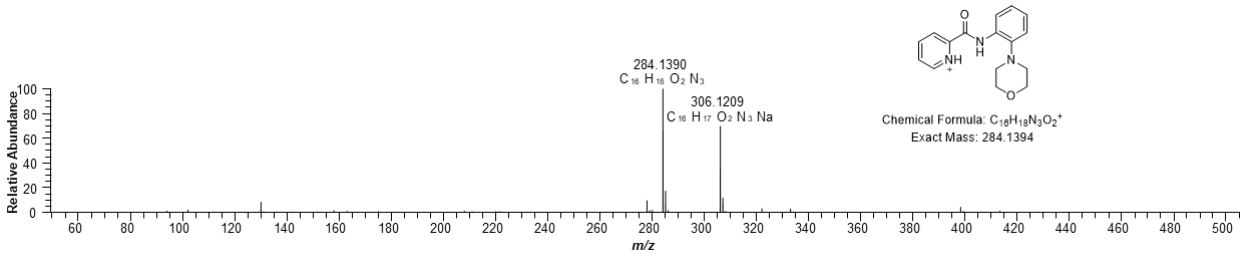

Fig. S34: HRMS of **3** after purification by silica gel flash chromatography ([M+H]$^+$at *m/z* 284.1390 and [M+Na]$^+$ at *m/z* 306.1209)

S9. Intended scope and prospective applications

The present study is primarily intended to demonstrate the utility of the nanoelectrospray microreactor platform for probing rapid reaction kinetics, capturing reactive intermediates, and obtaining mechanistic insight under conditions that are difficult to access in conventional bulk solution. The extremely small reaction volumes, rapid mixing and transport, and transient nature of the electrochemically generated Cu species are intentionally leveraged to enable time-resolved observation of short-lived intermediate and fast catalytic events.

The scalability of the electrochemical microreactor concept is shown via scale-up of in situ Cu-catalyzed electrochemical C–H amination in an electrochemical cell and has also been previously demonstrated by our group using Pd electrodes for electrochemical catalysis (J. Am. Chem. Soc. 2022, 144, 1306–1312). In that study, reaction conditions identified in the microreactor were successfully translated to preparative-scale synthesis, demonstrating that mechanistic insights obtained from the platform can inform scalable synthetic protocols when product formation is the primary objective.

In the present work, the emphasis is placed on mechanistic interrogation of transient Cu(I)-mediated processes. The primary advantage of the nanoelectrospray microreactor lies in its ability to access ultrafast reaction regimes and detect reactive intermediates that are difficult to observe, accumulate, or characterize under bulk conditions because of slower kinetics and competing pathways. At the same time, the broader applicability of the electrochemical microreactor concept was demonstrated through the successful scale-up of the in-situ Cu-catalyzed electrochemical C–H amination in an electrochemical cell.

References:

(1) Yang, Q.-L.; Wang, X.-Y.; Lu, J.-Y.; Zhang, L.-P.; Fang, P.; Mei, T.-S. Cu-Catalyzed Electrochemical C–H Amination of Arenes with Secondary Amines. *Journal of the American Chemical Society* **2018**, *140* (36), 11487-11494. DOI: 10.1021/jacs.8b07380.